Nano Research

Open Access

Review Article

Tandem electrocatalysts for CO_2 reduction to prepare multi-carbon products

Zaiming Chen[1,§], Xuewei Song[1,§], Tao Long[1], Yugang Yan[2], Fei Lv[3], Jing Ma[3], Shengpan Peng[3], Zhengwei Tong[3], Fangkun Fan[4], Rongfei Yu[5], Dafeng Yan[5] ✉, and Shenghua Chen[4] ✉

[1] *CHN Energy Zhejiang Ninghai Power Generation Co. Ltd, Ningbo 315612, China*
[2] *CHN Energy Zhejiang Electric Power Co. Ltd, Hangzhou 310020, China*
[3] *Nation Institute of Clean-and-Low-Carbon Energy, CHN Energy, Beijing 102209, China*
[4] *National Innovation Platform (Center) for Industry-Education Integration of Energy Storage Technology, School of Chemical Engineering and Technology, Xi'an Jiaotong University, Xi'an 710049, China*
[5] *Hubei Key Laboratory for Precision Synthesis of Small Molecule Pharmaceuticals and Ministry of Education Key Laboratory for the Synthesis and Application of Organic Functional Molecules and College of Chemistry and Chemical Engineering, Hubei University, Wuhan 430062, China*
§ *Zaiming Chen and Xuewei Song contributed equally to this work.*

Cite this article: *Nano Research*, **2025**, *18*, 94907270. https://doi.org/10.26599/NR.2025.94907270

ABSTRACT: Electrocatalytic CO_2 reduction reaction (CRR) is considered as a sustainable approach to converting CO_2 into high value-added chemicals, assisting the goal of carbon peaking and carbon neutrality. Electrochemical CRR can be easily regulated by controlling the electrocatalyst, electrolyte, and reactor to produce various chemicals. Among different products, multi-carbon (C_{2+}) products draw widespread attention for their high energy density and value along with complex reaction mechanisms. It is well recognized that *CO intermediate plays vital role in forming C_{2+} products and Cu is the only metal catalyst which can efficiently electro-reduce CO_2 to C_{2+} products. Therefore, researchers developed many strategies to increase the amount of *CO intermediate and further enhance the performance of C_{2+} products. Recently, designing tandem electrocatalysts consisted of Cu and the materials which can convert CO_2 to *CO intermediate has become a hotspot and achieved great achievements. In this review, we will summary the recent progress in tandem electrocatalysts for CO_2 reduction to prepare C_{2+} products, including the origin and fundamental mechanism of tandem electrocatalysis, the strategies of catalyst design, and regulation principles. In addition, some newest findings, like Cu tandem catalysts can achieve to produce C_{2+} products, are well introduced. Finally, the remaining challenges and prospects for future development are also proposed.

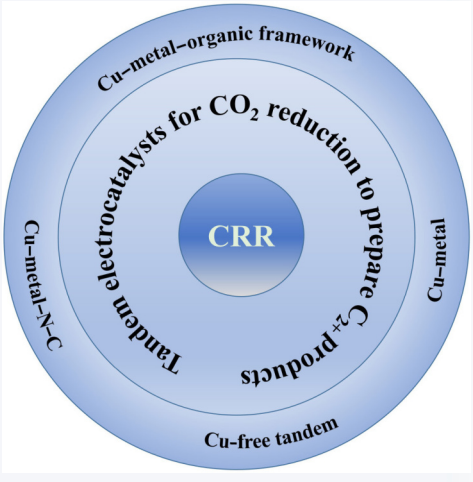

KEYWORDS: electrocatalytic CO_2 reduction, tandem electrocatalysis, multi-carbon products, electrocatalyst

1 Introduction

Since the Industrial Revolution, the massive emissions of CO_2 gas from the combustion of fossil fuels have caused serious environmental challenges [1–3]. It has become a worldwide issue to reduce net CO_2 emissions via various strategies, such as carbon sequestration, carbon recycling, and using renewable clean energy sources. Electrochemical technology can convert inert gases into valuable chemicals in ambient conditions with unique advantages and has drawn much attention recently [4–13]. Therefore, developing efficient electrocatalytic technologies driven by renewable energy to reduce CO_2 to hydrocarbon fuels shows great potential to mitigate emissions and recycle carbon loops [14–22]. By this way, it can not only store intermittent renewable energy but also produce valuable chemicals. Electrocatalytic CO_2 reduction reaction (CRR) can assist in generating C_1 products (HCOOH, CO, CH_4, and CH_3OH) and multi-carbon (C_{2+}) products (C_2H_4 and C_2H_5OH) via choosing specific catalysts [23–32]. Among different

Received: December 16, 2024; **Revised:** January 14, 2025
Accepted: January 22, 2025

✉Address correspondence to Dafeng Yan, dafengyan@hnu.edu.cn; Shenghua Chen, shenghchen@xjtu.edu.cn

products, C_{2+} products draw widespread attention for their high energy density and value along with complex reaction mechanisms. However, the selectivity, activity and stability of electrocatalytic CRR to form C_{2+} products are still in the initial stage and far away from industrial application [33–35].

Currently, Cu is well recognized as the only metal catalyst which can efficiently electro-catalyze CO_2 to C_{2+} products [36]. In addition, Cu metal shows very specific properties which can synthesize kinds of chemicals varying from C_1 products (HCOOH, CO, CH_4, and CH_3OH) [37–39] to C_{2+} products (C_2H_4 and C_2H_5OH) [40, 41]. The products selectivity can be greatly affected by the surface properties of Cu, such as defects, crystal facet, valence state, and heteroatom doping. Therefore, it is very difficult to design and control Cu-based catalysts to selectivity electro-reduce CO_2 to produce C_{2+} products with high activity and stability [42, 43]. Researchers from all over the world have developed various strategies, including defect engineering [44, 45], interface engineering [46, 47], surface modification, and so on, to enhance the performance of electrochemical CRR to form C_{2+} products [48, 49]. Electrochemical CRR to generate C_{2+} products is a process with multiple electron-proton transfer and C–C intermediate coupling steps, leading to an extremely complex reaction mechanism [31, 50, 51]. With the fast developments of nanotechnology and advanced characterization techniques, extensive research during the past decades has proved that *CO species is a key intermediate for C_{2+} products during the electrochemical CRR [52–54]. CO_2 molecules can be first converted into *CO intermediate adsorbed on suitable Cu surface and then *CO can be further reduced to C_{2+} products via C–C coupling [55–57]. Thus, it is well recognized that to increase the coverage of *CO on the catalyst surface is an effective strategy to promote the generation of C_{2+} products [58, 59]. Researchers can design tandem electrocatalysts which can *in-situ* produce *CO intermediate to enhance the performance of C_{2+} products, such as CuAu [60], CuAg [61], and Cu-NiNC [62].

Various effective CO production catalysts, such as Ag, Au, metal–N–C, have been developed and applied for electrocatalytic CRR to produce CO. For the tandem catalysts, researchers can develop various CO production catalysts and couple them with Cu-based materials. It contains mainly two species including active CO production catalysts and Cu species. With the fast development of tandem electrocatalysts, researchers have reported many preparation methods to synthesize the effective catalysts, such as co-reduction, pyrolysis, electrospinning, and physical mixture. The tandem electrocatalysts can take advantage of both CO production catalysts and Cu species to electro-reduce CO_2 to produce C_{2+} products effectively. Researchers can easily optimize the composition or structure and the relative proportion of two tandem catalysts to promote the coupling performance of C_{2+} products. The increased *CO intermediate produced by CO production catalyst can be further reduced and coupled to form C_{2+} products. Therefore, the tandem strategy can obviously enhance the performance of C_{2+} products for Cu-based catalysts. For example, Xie et al. reported that 1.4%Pd-Cu@$CuPz_2$ (Pz = pyrazole) tandem catalyst can achieve a high C_{2+} Faraday efficiency (FE) of 81.9% and C_{2+} alcohol FE of 47.5% with remarkable stability, which is much higher than that of $CuPz_2$, indicating the positive effect of the tandem strategy [63]. Li and co-workers designed a CuAg tandem catalyst to produce ethanol with the FE of 56.5%, which is much higher than that of bare Cu (less than 30%) [64]. It has become a research hotspot to combine a highly selective catalyst for CO with metal Cu to achieve tandem electrochemical CRR [65–68]. Very recently, even some Cu-free tandem electrocatalysts can also synthesize C_{2+} products with high efficiency [69]. However, a comprehensive and timely overview of tandem electrocatalysis is still lacking. It is urgent to provide a deep understanding of this tandem reaction process, highlighting the strategies of catalyst design and the regulation principles of tandem electrocatalysis to enhance the performance.

In this review, we will summary the recent progress in tandem electrocatalysts for CO_2 reduction to prepare C_{2+} products, including the origin and fundamental mechanism of tandem electrocatalysis, the strategies of catalyst design, and regulation principles. In each part, the detail mechanism is well discussed based on the experimental and calculated results. In addition, some newest findings, that Cu-free tandem catalysts can achieve to produce C_{2+} products, are well introduced. Finally, the remaining challenges and prospects for future development are also proposed.

2 Understanding the tandem electrocatalysis

Understanding the fundamental reaction mechanism of electrochemical CRR is crucial for purposefully enhancing the selectivity of C_{2+} products. Electrocatalytic CRR involves multi-electron and protons, resulting in an extremely complex process. Therefore, the surface properties play a vital role in regulating the type of products [14, 53, 70]. The adsorption strength and configuration of reaction molecular and intermediates determines the reaction directions [71–74]. For example, it is generally accepted that the *COOH intermediate tends to form CO, while *OCHO intermediate prefer to generate HCOOH. Considering the formation of C_{2+} products, *CO is recognized as a key reaction intermediate for C–C coupling. Thus, to increase the coverage of *CO should be a potential strategy to enhance the performance of C_{2+} products [58].

To reveal the importance of the coverage of *CO directly, Wang et al. systematically studied the effect of CO feed gas for electrocatalytic CRR to ethylene [75]. From their results, it can be concluded that the cross-coupling Langmuir–Hinshelwood type mechanism with the *CO intermediates deriving from both CO_2 and CO feed gas is the primary dimerization pathway (Fig. 1(a)). They took the isotope-labelled $^{12}CO_2$ and ^{13}CO co-feeds to uncover the origin of the C atoms in the product of ethylene, indicating the contribution of both CO and CO_2. As shown in Figs. 1(b) and 1(c), the C_2H_4 product formation rates were enhanced obviously compared to those of pure CO_2 and CO, proving the positive effect of directly inducing CO feed. Based on their findings, they further designed a tandem electrocatalyst which can electro-reduce CO_2 to produce internal CO co-feed instead of external CO_2 and CO feeds, which can increase the *CO coverages and promote the dimerization rates. Ni–N–C can produce CO *in-situ* and CuO_x nanoparticles (NPs) served as the sites for C–C coupling (Fig. 1(d)). By this tandem electrocatalyst strategy, C_2H_4 production rate can also be increased greatly (Fig. 1(e)), which is consist with the CO_2 and CO feed gas result. The enhanced performance compared to CuO_x indicated that the tandem electrocatalyst can produce CO internally and promote the coupling process.

Motivated by this tandem electrocatalyst idea, researchers can optimize various catalysts design to precisely control the *CO intermediate and C–C coupling process and further enhance the performance of C_{2+} products [63, 76–80]. In the following section,

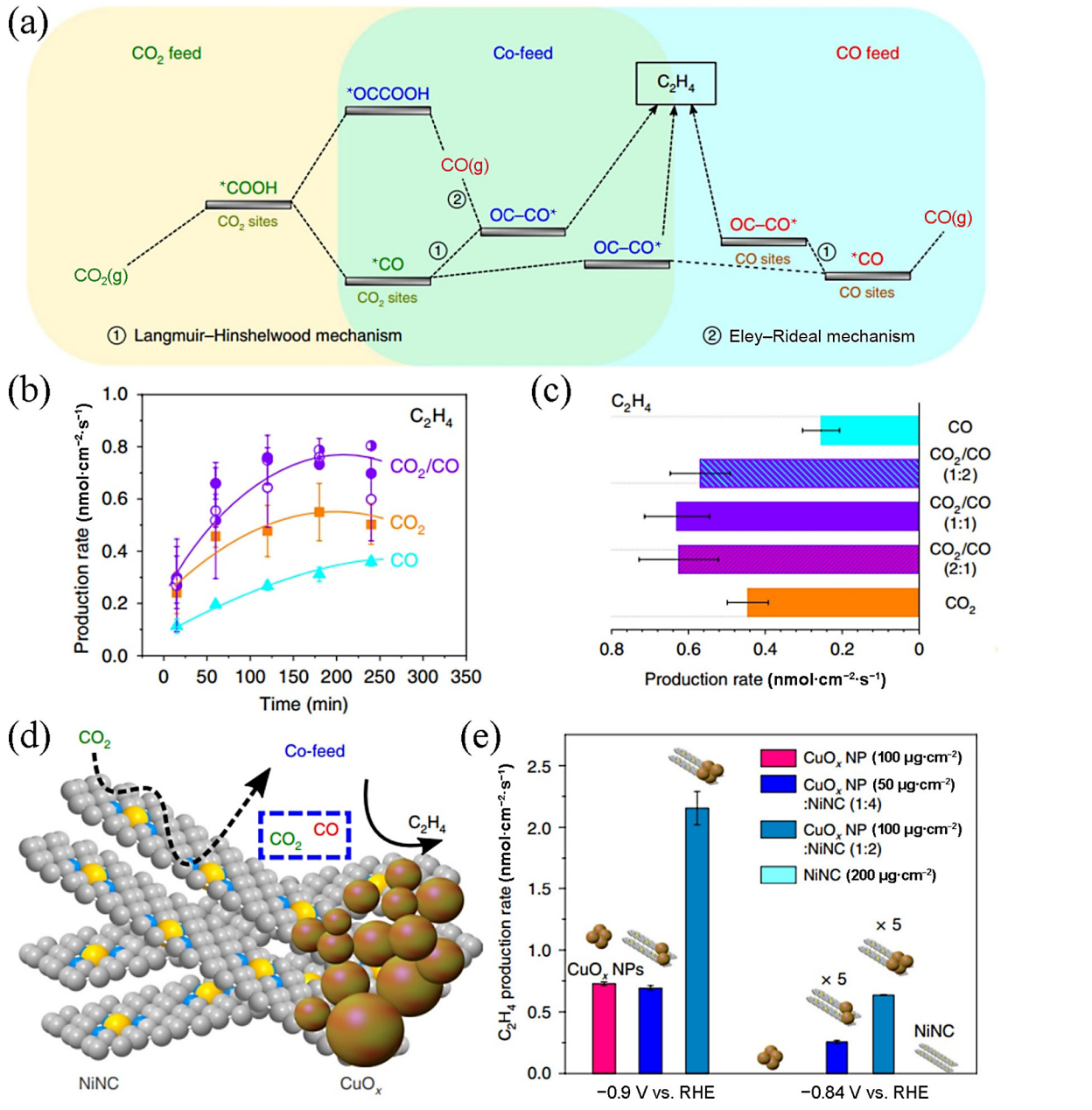

Figure 1 (a) The proposed possible dimerization pathways with intermediates in co-feed CO_2 and CO. (b) Time-dependent C_2H_4 product formation rates at −1.0 V vs. RHE. (c) C_2H_4 production rates at different feed conditions. (d) The tandem catalyst design combines NiNC and CuO_x NPs. (e) C_2H_4 production rate of different samples. Reproduced with permission from Ref. [75], © Wang, X. L. et al. 2019.

we will discuss the strategies of the tandem electrocatalyst design in detail.

3 Cu-based tandem catalyst design

The tandem electrocatalysts strategy should design multiple active sites including materials which can electro-reduce CO_2 to produce CO and Cu-based materials [81–83]. Recently, researchers have developed kinds of electrocatalysts which can selectively catalyze CO_2 to synthesize CO products with high efficiency, such as metal Au, Ag, and Zn, carbon-based metal–N–C, metal–organic framework (MOF) [24, 67, 84, 85]. Therefore, designing tandem electrocatalysts based on these efficient CO production catalysts and Cu shows great potential to develop optimized catalysts for the formation of C_{2+} products. In this part, we will induce and discuss recent findings according to the classification of tandem species for CO generation.

3.1 Metal materials

Some metallic catalysts, such as Ag and Zn, show high CO product selectivity to increase the amount of *CO intermediate and further promote the performance of electrochemical CRR to C_{2+} products [86–88]. Therefore, many novel findings have been achieved by combining these metallic catalysts with Cu-based materials. To further increase the unsatisfied performance, it is important to understand and optimize the synergy effect between Cu and induced metal like Ag. Gao et al. evaluated the formation of *CO intermediate and the subsequent spillover and hydrogenation

process for electrochemical CRR by *operando* Raman spectroscopy [89]. As shown in Fig. 2(a), they prepared the tandem CuAg catalyst by loaded Ag on Cu_2O nanowire via galvanic replacement reaction. It can be concluded from the electrochemical results that the tandem CuAg catalyst showed higher activity towards C_2H_4 indicated by the partial current density than that of pure Cu, indicating the positive effect of Ag (Fig. 2(b)). In addition, the tandem CuAg catalyst also showed enhanced FE of C_2H_4 shown in Fig. 2(d), which can be increased from 33% to 52%. It also showed good stability during long-term operation and the Faraday efficiency just decreased a little from 50% to 44% after 12 h electrolysis. However, considering the practical application, researchers are expected to evaluate the long-term stability at large current density by optimizing the electrolyzer cell and try to keep high performance for hundreds of hours. During the harsh condition of large current density, the active tandem species may undergo surface reconstruction, especially for Cu, and decrease the activity obviously. Therefore, it is also very important to develop various strategies to modify the surface properties of tandem catalysts to enhance the long-time stability. Most of the researches are still in the initial stage to promote the activity and selectively, and still far away from the industrial application for tandem catalysts. To reveal the reaction mechanism of the tandem CuAg catalyst, the authors took *operando* Raman spectroscopy at different potentials to track and compare the reaction intermediates during CRR. Comparing the Raman results of pure Cu and CuAg tandem catalyst (Fig. 2(c)), it can be deduced that CO intermediates underwent the desorption from Ag spillover to Cu sites and were further reduced to form hydrocarbons. Therefore, according to the electrochemical results and various characterizations, the possible mechanism for the formation of C_2H_4 on CuAg tandem catalyst was proposed (Fig. 2(e)). Both Cu and Ag can reduce CO_2 to CO and the CO generated on Ag sites would desorb result from its weak binding energy and reabsorb on the near Cu sites, which can increase the *CO intermediates concentration on Cu surface. And the increased *CO intermediates can lead to the high performance of C_{2+} products. The tandem catalyst strategy involves two different sites which can reduce CO_2 to CO first and then convert *CO intermediates to C_{2+} products via C–C coupling. It plays a vital role in controlling the amount and spillover of intermediates, the resorption of the intermediates and the further reduction and coupling of intermediates. To develop the tandem catalysts and promote their application, researchers can further design and optimize the tandem catalysts from the composition, structure and integration precisely to control the whole coupling process pertinently.

With the fast development of the nanotechnology and advanced instrument and equipment, researchers have successfully synthesized serious novel tandem catalysts to enhance the electrocatalytic CRR performance of C_{2+} products and could understand the reaction mechanisms and structure–activity relationship at atom level [50, 79, 90–93]. After understanding the process of tandem catalysis, we can know that both the surface coverage of adsorbed *CO and the adsorption energy of *CO on

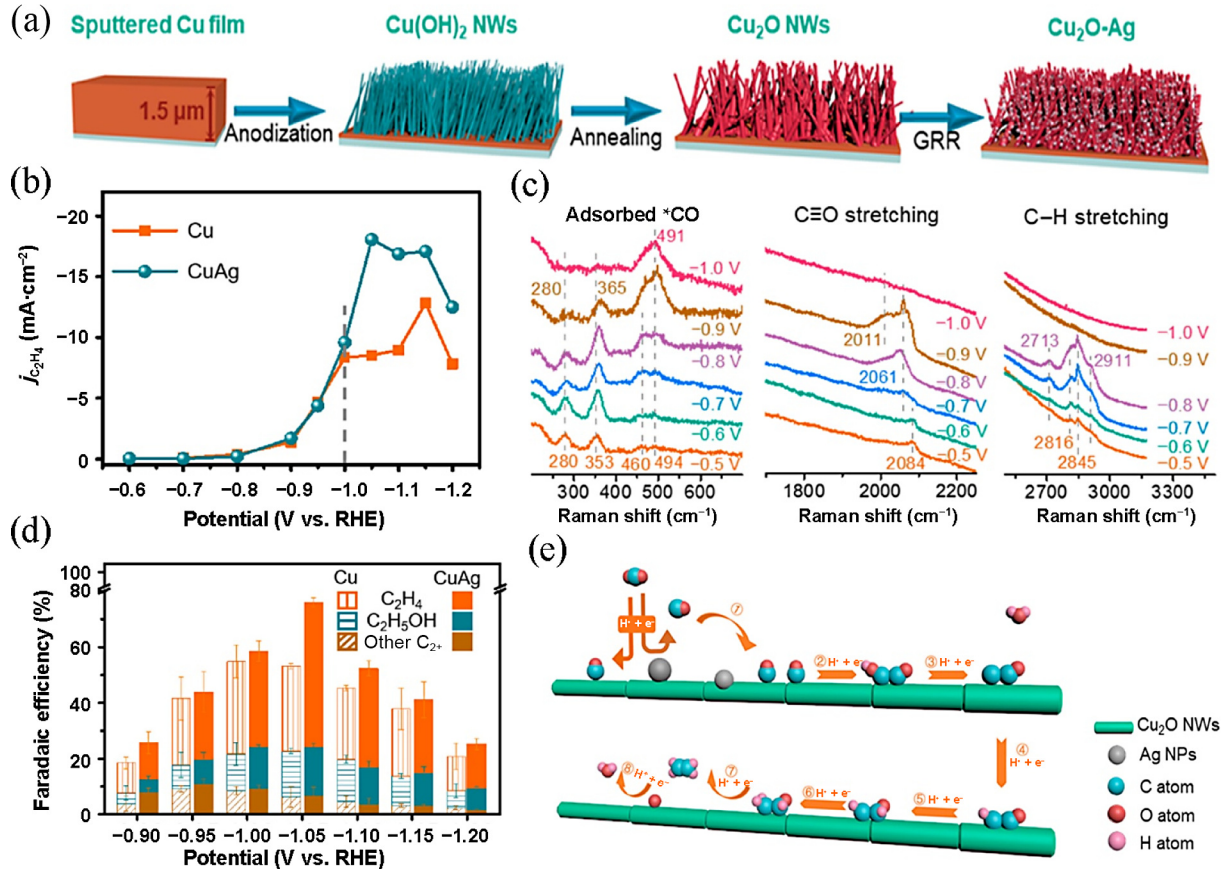

Figure 2 (a) Schematic route for the synthesis of Cu_2O and Cu_2O-Ag. (b) Partial current densities of C_2H_4 product. (c) *Operando* Raman spectra of CuAg catalyst for CRR at different potentials. (d) FEs of C_2H_4, C_2H_5OH, and other C_{2+} products. (e) Schematic mechanism for the formation of C_2H_4 on CuAg tandem catalyst. Reproduced with permission from Ref. [89], © American Chemical Society 2019.

the Cu surface affect the performance of C_{2+} products. But researchers focused more on the design of tandem catalysts to increase the coverage of *CO and ignored the optimization of the adsorption energy of *CO. Wu and co-workers designed and synthesized tandem catalyst to optimize both the coverage of adsorbed *CO and the adsorption energy of *CO, which was achieved by AgCu single-atom alloy (SAA) for C–C coupling site and Ag nanoparticles for the formation of CO locally (Fig. 3(a)) [94]. The Cu nanoparticle doped with Ag single-atom can obviously increase the adsorption energy of *CO on the surface of Cu sites, promoting the enhanced performance of C_{2+} products via C–C coupling. The atomic Ag doped into the Cu crystal lattice can be observed directly by aberration-corrected high-angle annular dark-field scanning transmission electron microscope (AC-HAADF-STEM) image shown as bright dots (Fig. 3(b)). From the electrochemical results shown in Fig. 3(c), typically, it can be seen that the designed AgCu SANP showed the highest C_{2+} FE of 94% ± 4% at the potential of −0.65 V vs. reversible hydrogen electrode (RHE) among the samples of Cu NP (56% ± 7%), AgCu SAA (78% ± 3%), and AgCu NP (73% ± 1%). Serial results showed that Ag nanoparticles can increase the local CO concentration, and the Cu doped with atomic Ag can promote the C–C coupling, which consists with expectation and indicates the ideal design of both the coverage and adsorption of *CO. Researchers are encouraged to consider the two factors together and develop more efficient tandem catalysts with satisfactory activity and stability.

For the strategy of tandem catalysts, it is obvious that the relative proportion of two catalysts can have a great effect on their performance of C_{2+} products [95]. The relative proportion of active species can adjust the coverage and utilization of *CO, influencing the coupling step [96]. In addition, it is well recognized that the electrocatalytic reactions are normally dynamic change and the prepared catalysts would undergo surface reconstruction [97–99]. Therefore, to study the relative proportion of the tandem catalysts and track the dynamic reconstruction during electrochemical CRR is strongly necessary. Recently, Zhang et al. evaluated the effect of the relative proportion of Cu and Ag and tracked the dynamic restructuring during working conditions, which can help others to understand the interfacial structure-steered product selectivity (Fig. 3(d)) [100]. They took systemic characterizations to reveal dynamic restructuring of different conditions to form interface structure with specific properties, which would steer product selectivity to generate different products. As shown in Fig. 3(e), the products showed much different with the change of the relative proportion of Cu and Ag. It can be concluded that the Cu-rich interface prefers to produce C_2H_4, while the main product moves to C_2H_5OH when increasing Ag content. Finally, it produces CO when the main component is Ag. The results indicated that the concentration of *CO intermediate can regulate the interfacial restructuring, and the Cu atoms can migrate onto the neighboring Ag to optimize the oxyphilic properties to determine the type of the products. In the future, researchers are expected to track the dynamic changes of both tandem catalysts and CO_2 reaction molecule based on serious *in-situ* characterization technologies, revealing the real reaction mechanism of tandem process and establish accurate structure–activity relationship.

As the electrochemical CRR would undergo dynamic restructuring inevitably, it would be great if we can utilize the advantage of the restructuring to induce the desired species *in-situ*. This restructuring strategy has been widely used in different electrocatalytic applications, such as oxygen evolution reaction, hydrogen evolution reaction (HER), and oxygen reduction reaction. We can control the restructuring process via the directions we want to form active species for a certain reaction by regulating the structure, composition, and crystal form of the pre-catalysts. Considering the situation of tandem catalysts for electrocatalytic

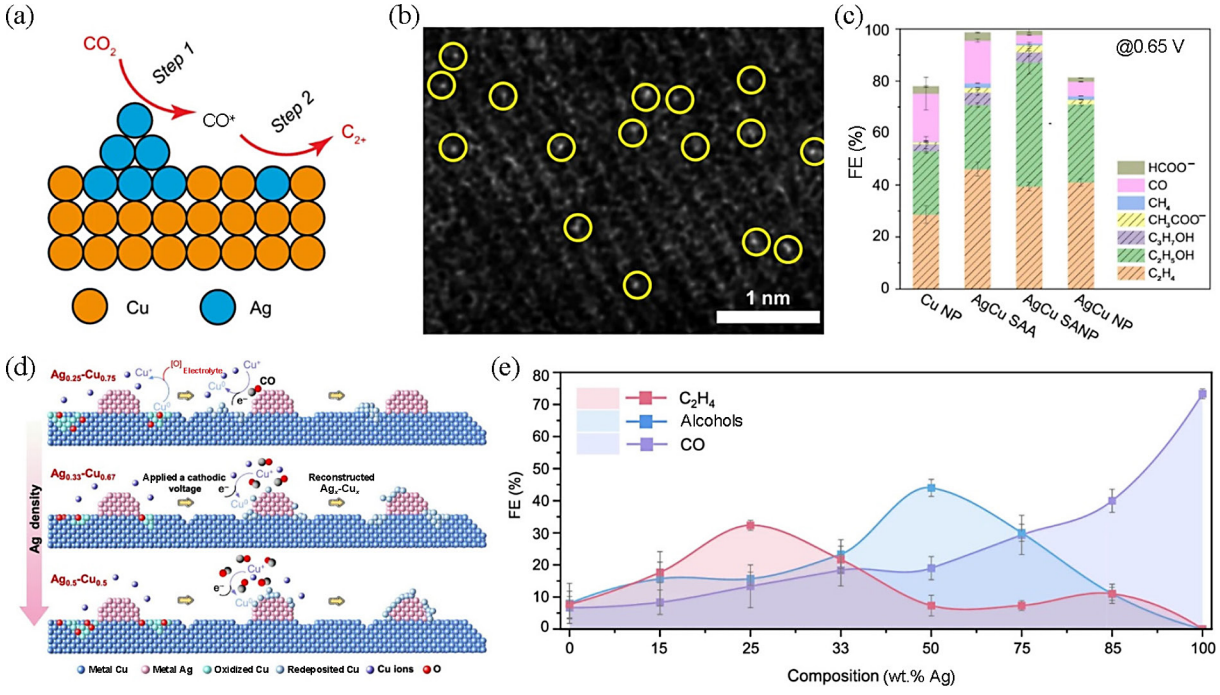

Figure 3 (a) Scheme of the tandem catalysis mechanism of AgCu single-atom alloy and Ag NP (denoted as AgCu SANP). (b) AC-HAADF-STEM image of AgCu SANP. (c) The comparison of FEs of different samples [94]. Reproduced with permission from Ref. [94], © Du, C. et al. 2023. (d) Scheme of reaction mechanisms of Ag–Cu heterostructures tandem catalysis with different Ag content. (e) The FEs of C_2H_4, C_2H_5OH and CO as a function of Ag content [100]. Reproduced with permission from Ref. [100], © Gao, X. Y. et al. 2024.

CRR, it is challenging to balance the dynamic structural evolution of two tandem species to construct highly active sites. Recently, Yang et al. developed ion mediated reconstruction strategy to balance the reconstruction rate of $CuO/AgIO_3$ tandem catalyst, which can promote both the steps for CO_2-to-CO and CO-to-C_{2+} products, showing a high C_{2+} products FE of 82% in acid electrolyte [101]. $CuO/AgIO_3$ tandem catalyst showed an overlapping nanosheets structure (Fig. 4(a)). They first compared the performance of Ag based the CO generation catalysts with different self-reducing ion (Fig. 4(b)). The results indicated that $AgIO_3$ showed the best CO selectivity in acidic electrolyte, delivering a FE of CO over 90% at high current density. Electro-adsorption method was used to evaluate the active surface areas, indicating the promotion effect of $AgIO_3$ (Fig. 4(c)). This ion mediated reconstruction strategy can form defective Ag due to rapid dissolution of iodate ions, which showed lower Gibbs free energy for *COOH than Ag and consisted with the electrochemical performance (Figs. 4(d) and 4(e)). Therefore, $AgIO_3$ is chosen as the CO generation part of the tandem catalysts.

Based on the discussion above, both the coverage of adsorbed *CO and the adsorption energy of *CO intermediate paly vital role in producing C_{2+} products for Cu-metal tandem catalysts. Therefore, when designing the Cu-metal tandem catalysts, researchers should focus on optimizing both the coverage of *CO and regulating the adsorption energy of *CO. In addition, the concentration of *CO intermediate can partly regulate the interfacial restructuring and affect the performance of C_{2+} products. Researchers must precisely optimize the Cu-metal tandem system via adjusting the surface electronic structure and the relative proportion of two tandem catalysts to get ideal coverage of adsorbed *CO and suitable adsorption energy of *CO.

3.2 Metal–N–C

Apart from metal catalysts like Au and Ag, metal–N–C, a typical type of single atom catalyst (SAC), has been widely studied as an efficient catalyst for CO formation from CRR [102–110]. The various metal–N–C based catalysts were developed via optimizing the metal center and coordination heteroatom, which can deliver high FE of CO above 90% at wide working potential window [31, 35, 111–113]. Therefore, metal–N–C based materials show great potential to designing tandem catalyst as the CO formation species for C_{2+} products formation from CRR. Metal phthalocyanine or metal porphyrin is classical single atom material with well-defined structure, which has been chosen as efficient catalysts for CO formation loaded on carbon-based supports [114–117]. Inspired by this suitable structure, researchers have developed various strategies to synthesize analogous M–N–C active species, including metal–organic framework derivative, molecular polymerization pyrolysis and so on [118–120].

Therefore, on the basis of M–N–C materials for CO formation, researchers can design many efficient tandem catalysts consisting of M–N–C and Cu-based materials for electrocatalytic CO_2 to generate C_{2+} products [121, 122]. However, it is still challenging to match the potential between CO formation and the C–C coupling step. Therefore, the concentration of *CO intermediate should match well with the C–C coupling potential window. To overcome this challenge, Liu and co-workers developed a Ni single atom catalyst which can produce CO efficiently at a wide range of potential window and combined with Cu to form tandem catalyst (Fig. 5(a)) [123]. They first prepared Ni single atom catalyst with the property of a wide CO generation-potential window and Cu catalyst with reductive state separately. And then the tandem catalyst was prepared via sufficient ultrasound Ni SAC and Cu catalysts. Ni K-edge absorption spectrum of Ni SAC indicated that Ni atoms remain with a +2 state, which is similar to those of nickel phtalocyanine (Ni Pc) and NiO (Fig. 5(b)). Fourier transformed extended X-ray absorption fine structure (EXAFS) spectra proved

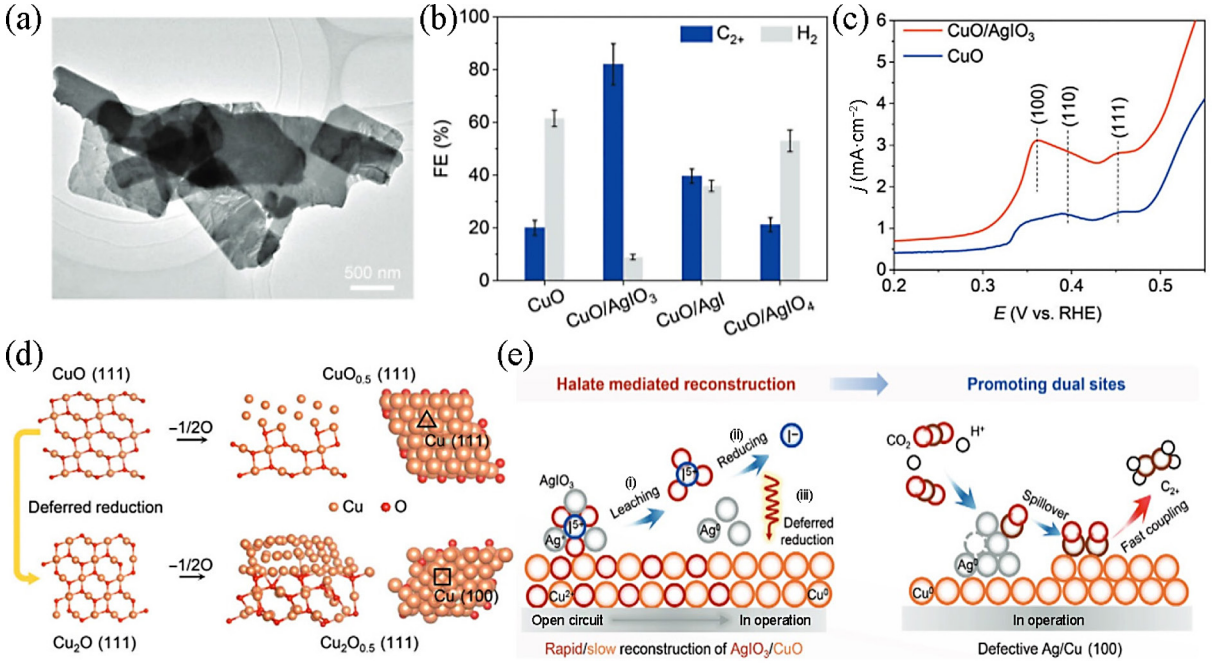

Figure 4 (a) Transmission electron microscope image of $CuO/AgIO_3$. (b) The comparison of FE of C_{2+} products for different samples at the current density of -1.0 A·cm^{-2}. (c) Electro-adsorption method to evaluate the active surface areas of CuO and $CuO/AgIO_3$. (d) Scheme of reducing process of CuO and Cu_2O. (e) Scheme of the reconstruction of $CuO/AgIO_3$ tandem catalyst and electrocatalytic CRR to produce C_{2+} products. Reproduced with permission from Ref. [101], © Wiley-VCH GmbH 2024.

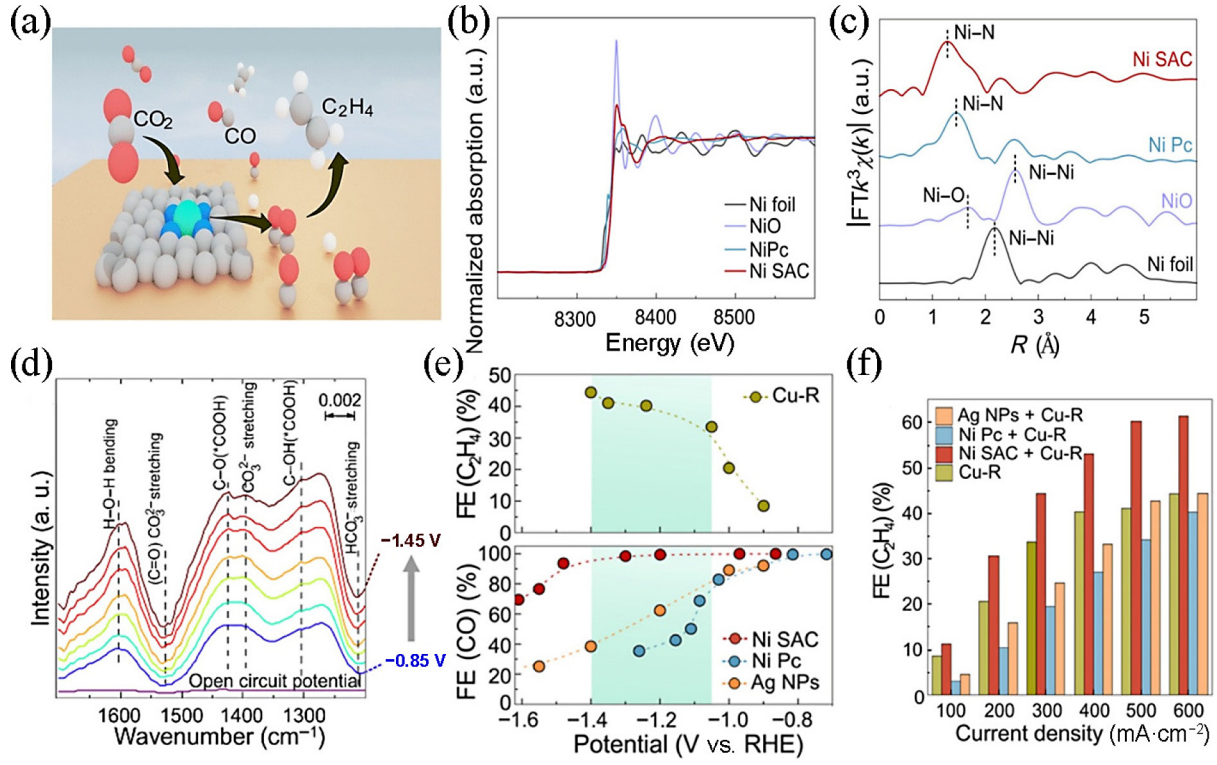

Figure 5 (a) Scheme of the tandem process for the formation of C_2H_4. (b) Ni K-edge X-ray absorption near-edge structure (XANES) spectra of and (c) Fourier transform spectra from EXAFS of Ni SAC and Ni Pc. (d) *In-situ* ATR-IR spectra within 1200–1700 cm^{-1} for Ni SAC during electrocatalytic CRR. (e) Potential matching between Cu and different CO formation catalysts. (f) The comparison of C_2H_4 FE of different tandem catalysts [123]. Reproduced with permission from Ref. [123], © Liu, M. et al. 2023.

the absence of Ni–Ni bonding in Ni SAC, showing the atomic dispersion of Ni atoms (Fig. 5(c)). They further took *in-situ* attenuated total reflectance-infrared (ATR-IR) spectroscopy during electrochemical CRR at different potential to evaluate whether Ni SAC can provide efficient *CO for C–C coupling (Fig. 5(d)). Compared to Ni Pc and Ag, Ni SAC showed higher signal of *COOH stretching modes, indicating the higher CO production rate of Ni SAC at wide potential. To stand out the importance of the match potential of tandem catalyst of Ni SAC and Cu, they first evaluated their electrochemical performance of CO and C_2H_4 independently. As shown in Fig. 5(e), the reductive Cu can produce C_2H_4 efficiently at the potential range of −1.4 to 1.05 V vs. RHE, while only Ni SAC can produce CO with high efficiency at the same range. Therefore, Ni SAC can match well with reductive Cu and provide efficient *CO for C–C coupling to form C_2H_4. For the advantage of the well match of Cu and Ni SAC, their tandem catalyst showed obviously enhancement of C_2H_4 performance than original Cu and other tandem systems. The optimized Cu/Ni SAC tandem catalyst can deliver nearly 60% of C_2H_4 FE at the current density of 500 $mA{\cdot}cm^{-2}$ (Fig. 5(f)). More researchers are expected to pay attention to the match degree of the tandem catalysts. By optimizing the independent species of tandem system, it can help to control the reaction intermediate and route to synthesize desired C_{2+} products.

Apart from the optimization of the component of tandem system, the spatial structure of tandem catalysts paly vital role in promoting the performance (both activity and stability) and application of CRR to C_{2+} products especially for the condition of large-scale current density. When considering the future application, it showed great potential to perform the reaction at the condition of acid and flow cell. Thus, the spatial structure of the tandem catalyst and the route of tandem would have great effects on the long-term activity and stability. Researchers are expected to optimize the tandem structure to avoid the agglomeration of active sites, keeping working for a long time at harsh conditions.

Recently, Chen and co-workers designed the structure of M–N–C catalyst for CO formation and optimized the tandem structure for acid electrochemical CRR in a flow cell [67]. They found that CoPc/C catalyst showed excellent CO selectivity in alkaline conditions but the FE of CO was limited to 70% at acid condition resulted from the agglomeration of Co. They try to avoid the agglomeration by preparing a strongly interaction hollow carbon (HC) support and achieve CO production with high efficiency at acid condition (Fig. 6(a)). The formed CoPc@HC catalyst has a hollow structure and CoPc keeps independent without agglomeration. Then they prepared a tandem electrode consisting of the C–C coupling catalyst Cu followed by an upper layer of CO generation catalyst CoPc@HC (Fig. 6(b)). According to the electrochemical CRR performance results, the optimized the CoPc@HC/Cu tandem catalyst showed much better performance on C_{2+} products than that of single Cu electrode, which can deliver a total 80% FEs of C_{2+} products at high current density of 800 $mA{\cdot}cm^{-2}$, indicating the positive effect of the tandem system (Fig. 6(c)). The CoPc@HC/Cu tandem electrode exhibited a H_2 FE below 10% while Cu electrode showed a H_2 FE over 35% (Fig. 6(d)). CoPc@HC can generate a CO rich environment for the Cu electrode to suppress the HER and enhance the performance of C_{2+} products. The density functional theory (DFT) results indicated that the CoN_4–C/Cu model structure reduced the reaction energy required for C–C coupling by about 0.11 eV compared to that of Cu electrode and changed the reaction pathway for the

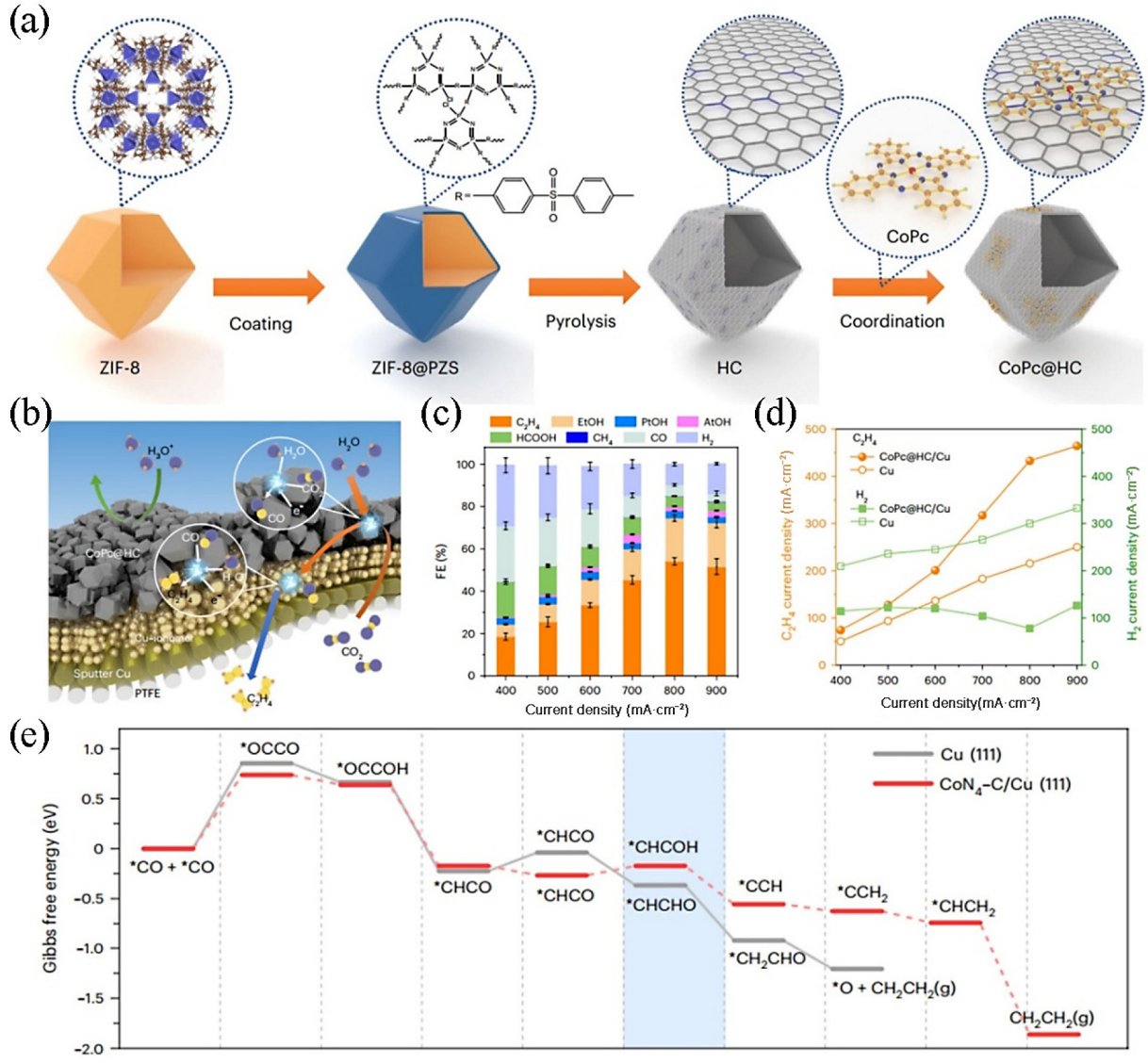

Figure 6 (a) Scheme of the synthesis process of CoPc@HC for CO generation. (b) Schematic of the spatially tandem strategy in acid condition. (c) FE values of different CRR products on the tandem catalyst of CoPc@HC/Cu. (d) The comparison of partial current densities of C_2H_4 and H_2. (e) The comparison of free energy diagram of CRR on CoN_4–C/Cu tandem and Cu electrodes. Reproduced with permission from Ref. [67], © Chen, Y. J. et al. 2023.

hydrogenation of *CCO to form C_2H_4 (Fig. 6(e)). The designed tandem catalyst for acidic CRR system can achieve a single-pass carbon efficiency (SPCE) of 90% along with a total C_{2+} FE of 76% and a C_2H_4 FE of 55% at a high current density of 800 mA·cm^{-2} and can keep nearly no change after 12 h operation.

For the Cu–metal–N–C tandem system, it is also very important to optimize the coverage of adsorbed *CO and the adsorption energy of *CO intermediate. The long-term stability for carbon-based materials should be considered especially at acid conditions. Researchers are expected to optimize the tandem structure to avoid the agglomeration of metal species via various strategies like confinement effect, porous structure. To design effective CO production metal–N–C catalyst at wide potential window can ensure the well match with the C–C coupling potential window, achieving electrocatalytic CRR to produce C_{2+} products efficiently.

3.3 Metal–organic framework

Metal–organic frameworks constructed by metal nodes and organic ligands, are an emerging class of porous crystalline materials with remarkable structural flexibility, offering a highly versatile platform for the incorporation metal atoms to design tandem catalysts [124–126]. In the tandem catalysis of metal-based MOFs, the electrocatalytic CRR occurs on the surface of the primary catalyst and then reacts continue within the pores of MOF or the metal-MOF interface to obtain further reduced products [127, 128]. Currently, Cu-based MOFs are the most selective tandem catalysts for electrocatalytic CRR to C_{2+} products [129–131]. Accordingly, the recently reported efficient strategies for fabricating selective Cu-based MOFs tandem catalysts to enhance C_{2+} products formation will be discussed in this section.

The C–C coupling through *CO dimerization or other intermediate coupling to generate C_{2+} products requires at least two active sites close enough to each other, guaranteeing the adjacent adsorption of reactive intermediates [132]. The Cu-based MOFs with rich adjacent dual active sites can effectively facilitate C_{2+} product formation through a synergistic tandem strategy. Zhang et al. successfully synthesized boron-imidazolate framework nanosheet catalysts with dimer Cu units (BIF-102NSs) and isolated

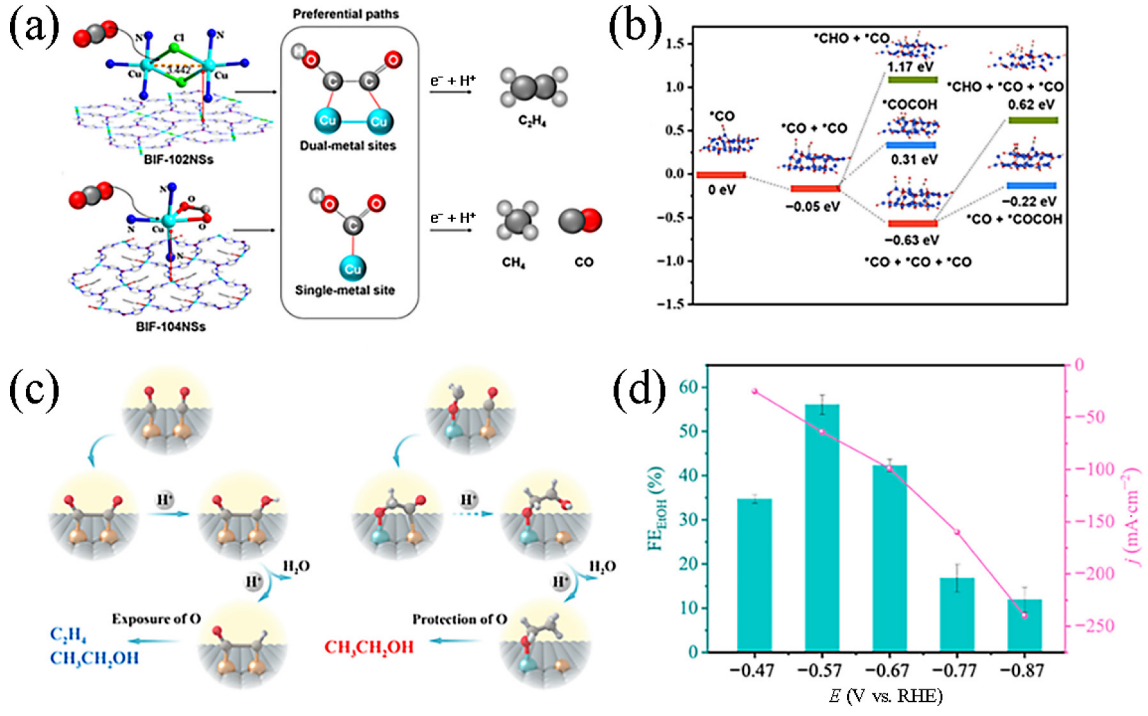

Figure 7 (a) Coordination environment of BIF-102NSs and BIF-104NSs and the illustration showing the preferential reaction pathways of different model systems. Reproduced with permission from Ref. [133], © Wiley-VCH GmbH 2021. (b) The energy diagram for the adsorption of one, two, or three *CO and the conversion of *CO-to-*CHO or *CO-to-*COCOH on the Cu_2O (111) surface. Reproduced with permission from Ref. [134], © Wiley-VCH GmbH 2024. (c) Proposed reaction paths for yielding C_2H_4 vs C_2H_5OH on the surface of conventional homometallic Cu–Cu dual sites (left) and heterometallic Sn–Cu dual sites (right). (d) FE of C_2H_5OH values at different potentials by CuSn–HAB. Reproduced with permission from Ref. [135], © American Chemical Society 2023.

Cu sites (BIF-104NSs), respectively [133]. As shown in Fig. 7(a), BIF-102NSs with adjacent dual Cu active sites can synergistically adsorb CO_2 molecules, facilitating subsequently C–C coupling between the CO_2 molecules from the adjacent Cu sites. Notably, BIF-104NSs achieved a high C_2H_2 FE of 11.3%, which is 3.2-fold enhancements of its single-metal counterparts (BIF-104 FE of 3.55%). Adjacent dual active sites in Cu-based MOFs with weak adsorption of *CO increase local *CO concentration, benefiting *CO transfer to another active sites for subsequent C–C coupling steps. Li at al. constructed a tandem catalyst for C_2H_4 production via the template-directed polymerization of ultrathin Cu(II) porphyrin (CuPor) organic frameworks (CuPOF) incorporating atomically isolated Cu(II) porphyrin and Cu(II) bipyridine (CuBpy) dual active sites on a carbon nanotube (CNT) scaffold, then Cu_2O nanoparticles were dispersed on the CNT scaffold, which was denoted as CuPOF-Bpy/Cu_2O@CNT [134]. Theoretical calculations revealed that *CO interaction energy for the CuPor sites and CuBpy in the CuPOF Bpy/Cu_2O@CNT only −0.008 and 0.009 eV. These small values suggest that the dual active sites can efficiently reduce CO_2 to *CO which subsequently transferred to nearby Cu_2O sites. As shown Fig. 7(b), the energy barriers for C–C coupling gradually decrease with the increase in *CO on Cu_2O sites. Accordingly, CuPOF Bpy/Cu_2O@CNT achieved a high FE of 71.0% for C_2H_4 formation at 1.1 V vs. RHE. It should be noticed that manipulating the types of dual active sites in Cu-based MOFs tandem catalyst is extremely important for generation of target products. As shown in Fig. 7(c), the key intermediate *CO–*COH for C_2H_4 and ethanol production tends to adsorb with each C atoms at homometallic Cu–Cu dual sites [135]. This adsorption mode results the exposes the C–O bonds, promoting the hydrogenation of O atoms and leading the cleavage of C–O bonds, ultimately yielding C_2H_4 as the product rather than other C_{2+} products. Liao et al. successfully synthesized a MOF with unprecedented heterometallic Sn–Cu dual sites (CuSn–HAB, HAB = hexaiminobenzene). As shown in Fig. 7(c), introducing Sn atoms with stronger affinity for O atoms in CuSn–HAB makes key intermediate *OCH_2 adsorb with O atom on Sn sites rather than C atom, which subsequently couples *CO formed on adjacent Cu sites [135]. Consequently, CuSn–HAB with hetermetallic Sn–Cu dual sites achieved an impressive FE of 56% for ethanol (Fig. 7(d)). The same situation can also be observed for PdCu@$CuPz_2$ catalysts with heterometallic Cu–Pd dual sites developed by Gou et al via embedding dispersive CuO_x and PdO dual nanoclusters into the MOFCuPz_2 [63]. The oxophilicity of Pd sites can stabilize the key intermediate *CH_2CHO and thus alter the reaction pathway toward ethanol production. Consequently, the 1.4% PdCu@$CuPz_2$ achieved a high FE of 47.5% for C_2H_5OH.

Cu-based MOFs with tunable ligands allow precise control of the local environment and electron properties of Cu active sites, thereby enabling the finely tuning the selectivity of electrocatalytic CRR for C_{2+} products. Chowdhury et al. explored the effect of different ligand environments in two-dimensional (2D) MOFs using copper naphthalenedicarboxylate (Cu-UNDC) and copper benzenedicarboxylate (Cu-UBDC). X-ray photoelectron spectroscopy (XPS) revealed that the changing of ligands made Cu-UNDC and Cu-UBDC with electronic environment, significantly changing the selectivity toward C_{2+} products [136]. As shown in Fig. 8(a), Cu-UNDC exhibited a higher FE of 24.3% for C_{2+} products compared to that of Cu-UBDC (13.2%). Modification of ligands with different side groups can also effectively regulate selectivity. Indra et al. systematically studied the effect of different functional ligand side groups on the CO_2RR selectivity using Cu

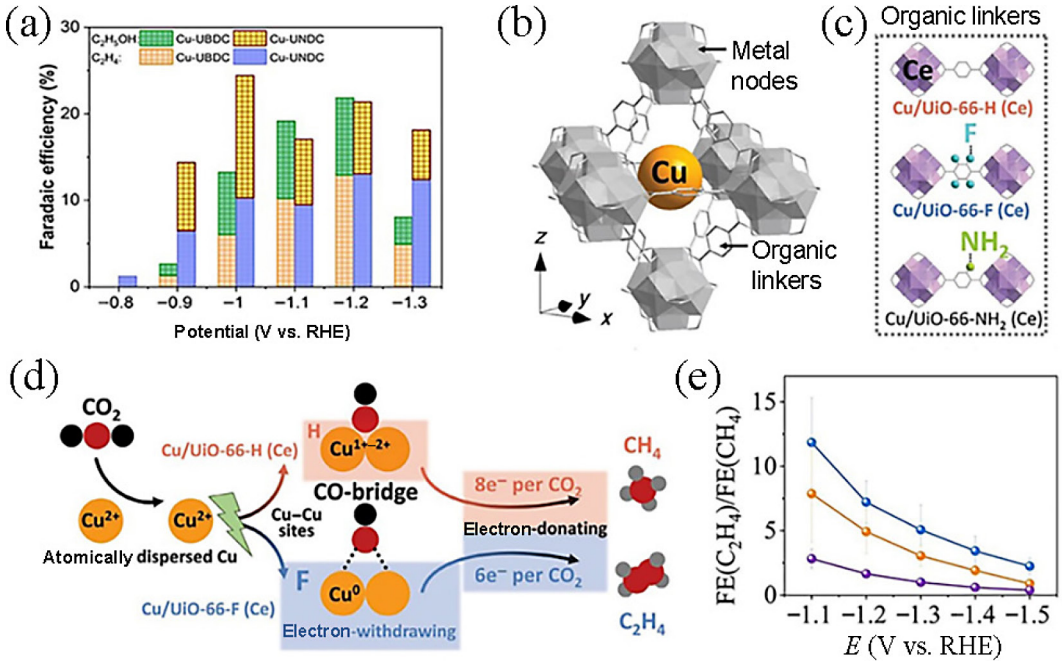

Figure 8 (a) FE of Cu-UNDC and Cu-UBDC toward C_{2+} products at different potentials. Reproduced with permission from Ref. [136], © American Chemical Society 2023. (b) Structure illustration of Cu/UiO-66-L (M). (c) H, F, and NH_2 are selected as the functional groups of the organic linker for Cu/UiO-66-L (Ce), respectively. (d) Mechanistic description of CH_4 and C_2H_4 formation for Cu/UiO-66-H (Ce) and Cu/UiO-66-F (Ce), respectively [137]. Reproduced with permission from Ref. [137], © Sun, M. X. et al. 2024. (e) Potential-dependent C_2H_4/CH_4 FE for MAF-2ME (blue), MAF-2E (orange), and MAF-2P (purple). Reproduced with permission from Ref. [138], © Wiley-VCH GmbH 2022.

incorporated UiO-66 composite catalysts (Cu/UiO-66-L (Ce)), where L represent side groups of 1,4-benzenedicarboxylic acid (BDC) linkers (Figs. 8(b) and 8(c)) [137]. *In-situ* Raman and X-ray absorption spectroscopy (XAS) revealed that functionalization with F exhibited a strong electron-withdrawing effect on BDC, facilitating electron accumulation and aiding the reduction of Cu^{2+} to Cu^0 in Cu/UiO-66-H (Ce). As shown in Fig. 8(d), Cu/UiO-66-F (Ce) with lower Cu valence is more capable of producing C_{2+} product compared to Cu/UiO-66-H (Ce). Consequently, Cu/UiO-66-F (Ce) preferentially generates C_{2+} products with a high FE of 44% for C_2H_4, while Cu/UiO-66-H (Ce) favors the production of C1 products, achieving a FE of 58% for CH_4, highlighting the role of ligand modification in selectivity regulation. Adjusting the size of ligand side groups provides an additional strategy for selectivity control. Zhou et al. successfully constructed Cu(I)-based metal azolate frameworks (MAFs) with different sizes of ligand side groups, namely MAF-2ME (3,5-dimethyl-1,2,4-triazole, with methyl side groups), MAF-2E (3,5-diethyl-1,2,4-triazole, with ethyl side groups), and MAF-2P (3,5-dipropyl-1,2,4-triazole, with propyl side groups) [138]. Theoretical calculations revealed that larger ligand side groups increase steric hindrance, making the framework less flexible, thus hindering the binding of two CO intermediates for C–C coupling to produce C_2H_2. As shown in Fig. 8(e), increasing the size of the ligand side groups greatly reduces C–C coupling, resulting in a selectivity shift from C_2H_4 to CH_4. This result highlights the critical role of ligand side group size in controlling electrocatalytic CO_2RR selectivity.

Changing the coordination number of Cu active sites can significantly influence the electron structure of Cu sites and impact the adsorption of key intermediates, steering the products selectivity greatly [139]. Therefore, it is essential to discuss coordination engineering for selectivity regulation in Cu-based MOFs tandem catalysts. Wang et al. constructed a novel 2D MOFs with planar asymmetric N/O mixed coordinated CuN_1O_3 unit (BIT-119) [73]. As shown in Fig. 9(a), compared to Cu-thioquinolinone (Cu-THQ) with coordinated Cu–O_4 units. BIT-119 exhibits a higher d-band center, indicating an enhanced adsorption capacity for key reaction intermediates. Free energy diagrams (Fig. 9(b)) further revealed that BIT-119 boosts the co-adsorption of two *CO species, facilitating the C–C coupling to produce C_{2+} products. Notably, BIT-119 can achieve a high C_{2+} FE above 60%. Undercoordinated Cu species in Cu-based MOFs can also enhance the adsorption of key intermediates promoting C–C coupling greatly. Zhang et al. constructed Cu-MOFs with linker vacancies (UC-Cu-BTEC) as efficient CO_2RR electrocatalysts for C_{2+} production [140]. *In-situ* XAS and Raman spectroscopy revealed that detaching partial ligands of UC-Cu-BTEC entailing the Cu dimer distortion and the emerging abundant undercoordinated Cu sites, which significantly improves the *CO coverage and stabilizes key C_2 intermediates, thus promoting C–C coupling. As shown in Fig. 9(c), UC-Cu-BTEC achieved a high FE of 77.2% for C_{2+} products, significantly outperforming the pristine MOF (Cu-BTEC). Altering the coordination environment of Cu active sites offers an efficient strategy for selectivity regulation. A novel "reduction–cleavage–recrystallization" method is developed by Xu et al. to transform the Cu(II)-trimesic acid (BTC) framework into a Cu(I)-BTC structure with rich free carboxyl groups in the secondary coordination environment (SCE) [141]. The coordination environment optimize in Cu(I)-BTC significantly enhances the dimerization of *CO intermediates and hinders the hydrogenation of *CO intermediates, enabling Cu(I)-BTC achieved a high FE of 57% for C_2H_4.

Metal–organic framework, with adjustable metal center and organic ligand, can serve as ideal platform to conduct tandem catalysts for C_{2+} products. The long-term stability of metal–organic framework based tandem catalysts is a great challenge at the

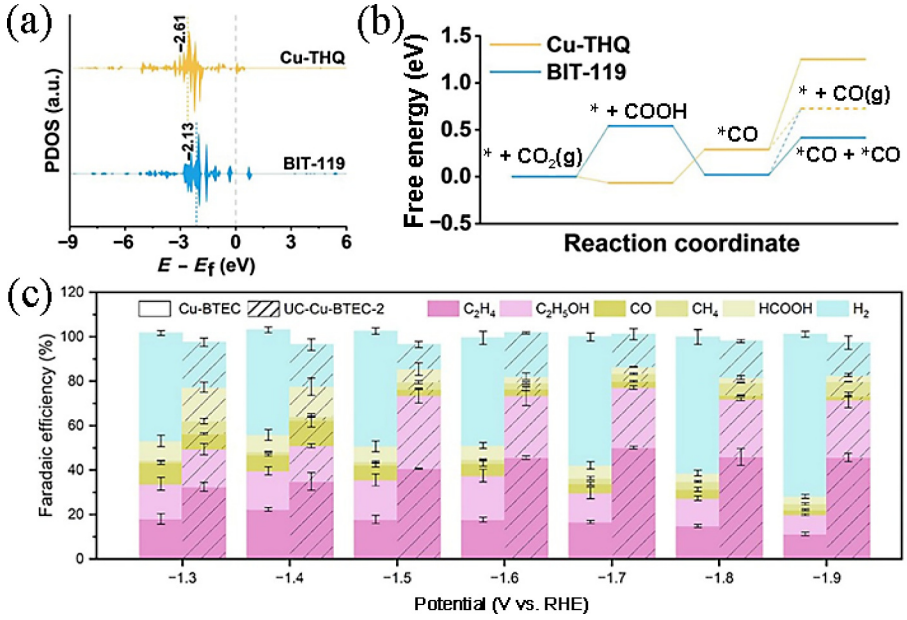

Figure 9 (a) Projected partial density of states of Cu-3d orbital for Cu-THQ and BIT-119. (b) Free energy diagrams for CRR through CO_2-to-CO and CO_2-to-2*CO pathway on Cu-THQ and BIT-119. Reproduced with permission from Ref. [73], © Wiley-VCH GmbH 2024. (c) A comparison of the FE of C_{2+} products on Cu-BTEC, UC-Cu-BTEC, and CuO_x. Reproduced with permission from Ref. [140], © Elsevier B.V. 2024.

condition of strong acid and alkaline. The strategies of surface and interface engineering can be applied to avoid the destruction of the main body of metal–organic framework. Researchers are expected to take advantage of metal–organic framework to promote gas diffusion and mass transfer to enhance the performance.

4 Newest Cu-free tandem catalysts

Tandem catalysts, as an effective catalytic strategy, significantly enhances the selectivity and efficiency of chemical reactions by integrating multiple catalytic steps within a single reaction system. In the field of electrocatalytic CRR, the application of tandem catalysts not only aids in mitigating greenhouse gas emissions but also promotes the production of high-value-added chemicals, thereby playing a crucial role in advancing sustainable chemistry and energy conversion technologies. Currently, apart from Cu-based tandem catalysts we discussed above, only a limited number of tandem catalysts are capable of catalyzing the reduction of CO_2 to produce C_{2+} products. Therefore, there is a pressing need to develop novel Cu-free tandem catalysts to enhance our understanding and improve the capability of producing high-value hydrocarbons and oxygenates from electrochemical CRR. Zhou et al. proposed a new type of internal tandem catalyst with two neighboring single-atom active sites, enabling the directional migration of adsorbed intermediates between adjacent binding centers through a feasible configuration transition [142]. This transition is driven by the affinities of C and O atoms in intermediates on the two binding centers of the internal tandem active sites. The Co–N–Cr neighboring single-atom system was discovered for efficient CH_4 formation towards electrocatalytic CRR, with remarkably low thermodynamic energy barriers of 0.35 eV for the entire pathway and kinetic activation energy of 0.09 eV for intermediate migration. Figure 10(a) shows the free energy diagrams and geometrical structures of CRR to CH_4 on Co sites (stage I, Co dominant) and M sites (stage II, M dominant) of Co–N–M (M = Cr, Mn, and Fe) in the inner tandem process. Wang and co-workers successfully synthesized cobalt phthalocyanine and zinc-nitrogen-carbon tandem catalyst, which can produce CH_4 effectively [143]. In this tandem strategy, CoPc can not only produce CO *in-situ* but also enhance the availability of *H over adjacent N sites in Zn–N–C, which is the key to achieve the high CH_4 production rate. And this tandem process is much different to the Cu-based system. However, it is still challenging to produce C_{2+} products via electrochemical CRR with Cu-free tandem catalysts.

Recently, Liu and co-workers reported a novel tin-based Cu-free tandem electrocatalyst, which can deliver a high C_2H_5OH FE of up to 82.5% at the potential −0.9 V vs. RHE [69]. This tandem catalyst is primarily composed of SnS_2 nanosheets and single Sn atoms coordinated with three oxygen atoms anchored on a three-dimensional (3D) carbon support via a local SnO3 cluster named Sn_1-O3G. The synthesis process of the SnS_2/Sn_1-O3G catalyst is shown in Fig. 10(e) in detail. The 3D carbon support is derived from ethylene deposited on an HY zeolite framework at 950 °C, ensuring a large surface area and efficient mass transport for electrocatalytic process. The subsequent solvothermal reaction at the condition of 200 °C for 20 h leads to the formation of SnS_2/Sn_1-O3G, using $SnBr_2$ and thiourea as precursors for Sn and S, respectively. The electrochemical performance of the SnS_2/Sn_1-O3G catalyst is characterized using linear sweep voltammetry (LSV) and chronoamperometry (CA) in a CO_2-saturated 0.5 M $KHCO_3$ solution. Figures 10(b) and 10(c) displayed the FE and partial current density of different products results, respectively, demonstrating its exceptional performance with an ethanol FE of up to 82.5% at −0.9 V vs. RHE. The high performance of the designed SnS_2/Sn_1-O3G to C_{2+} products is even comparable to the best of Cu-based tandem catalysts. It can also keep the excellent performance over 70% selectivity across a wide potential range of −1.3 to −0.6 V vs. RHE. The stability test results shown in Fig. 10(d) indicated that the catalyst can retain 97% of its initial activity after 100 h of continuous operation at a high geometric current density of 17.8 mA·cm^{-2}.

To further reveal the mechanism of the inspiring result with Cu-free tandem catalyst, they took systematically experimental and calculated methods to prove the incredible electrochemical performance of C_{2+} products and the mechanism of C–C coupling. The experiments indicated that SnS_2 nanosheets can first produce formate intermediates, while Sn_1-O3G sites generate *OCO(OH) bicarbonate intermediates, followed by C–C coupling to form C_2H_5OH at active centers comprising Sn and O atoms (Fig. 10(f)). DFT calculations further supported the proposed mechanism, showing that Sn atoms at Sn_1-O3G sites bind with *CHO

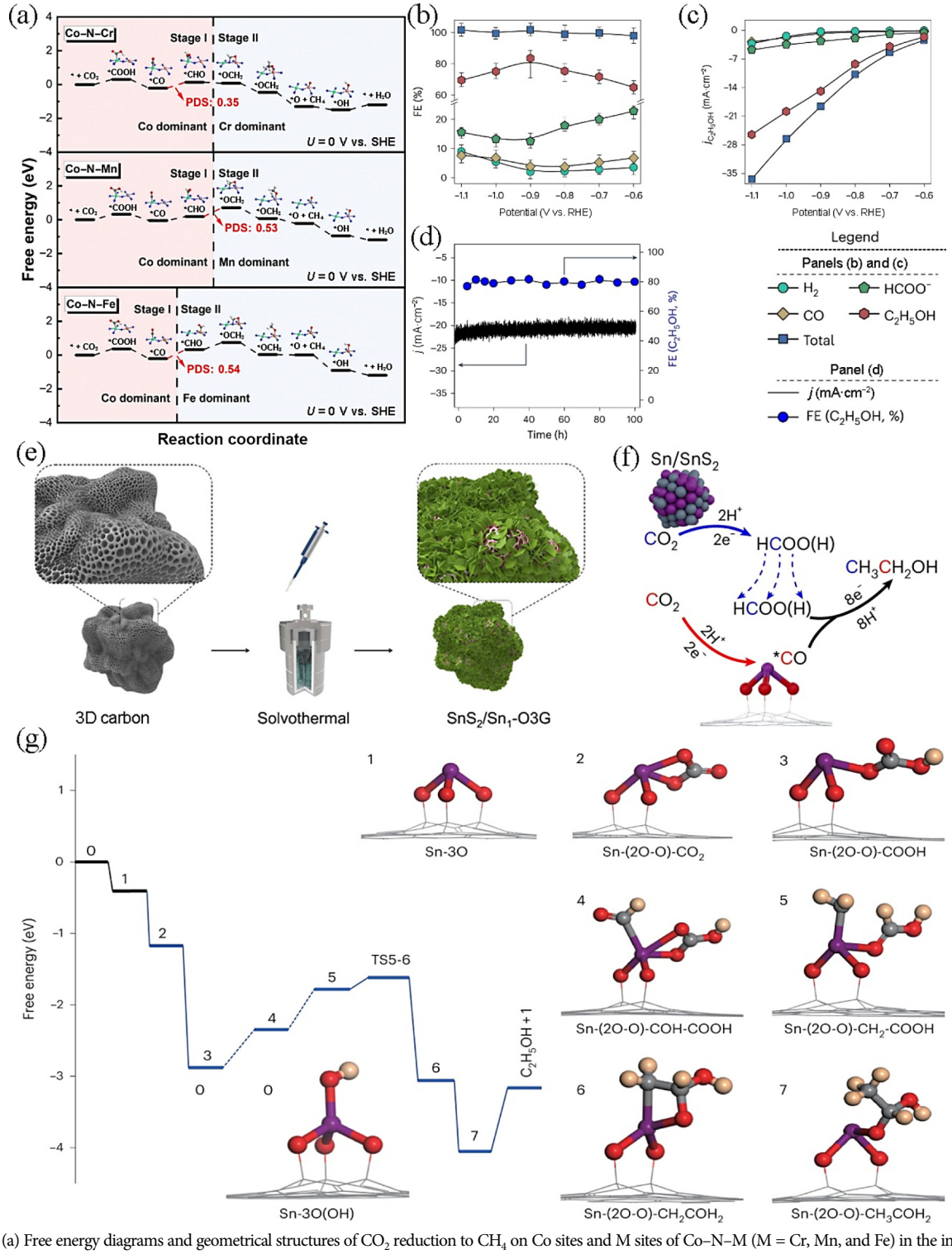

Figure 10 (a) Free energy diagrams and geometrical structures of CO_2 reduction to CH_4 on Co sites and M sites of Co–N–M (M = Cr, Mn, and Fe) in the inner tandem process. Reproduced with permission from Ref. [142], © The Royal Society of Chemistry 2023. (b)–(d) The CO_2RR performance of the SnS_2/Sn_1-O3G tandem catalyst. (b) FE values and (c) partial current density and total current density of different products. (d) Stability test. (e) A schematic illustration showing the procedure to prepare SnS_2@Sn_1-O3G. (f) A schematic illustration the cascade reaction of CO_2 reduction to C_2H_5OH over SnS_2/Sn_1-O3G. (g) Reaction energy profiles and the corresponding intermediate structures (0 to 7) for the formation of C_2H_5OH on the tandem catalyst Sn_1-O3G. Reproduced with permission from Ref. [69], © Ding, J. et al. 2023.

intermediates, while O atoms bind with *CO(OH) intermediates, thus promoting the formation of C–C bonds to form C_2H_5OH. The reaction energy profiles and the corresponding intermediate structures (0 to 7) for the formation of C_2H_5OH via the CRR on the Sn_1-O3G catalyst are shown in Fig. 10(g), further confirming the proposed mechanism.

Research on Cu-free tandem catalysts is still in its initial stage. More efficient catalysts are expected to be developed with stringent requirements to achieve electrocatalytic CRR to C_{2+} products. Further exploration and optimization novel tandem catalysts in this area require increased attention from researchers. Particularly, the development of more efficient Cu-free tandem catalysts is of significant importance in the field of CRR to C_{2+} products, which can greatly expand the potential of the design of tandem catalysts and promote the application. Sn-based catalysts offer a new pathway to improve the selectivity of target products by utilizing different active centers and potentially new reaction pathways.

Nowadays, it is still very difficult to conclude which elements or design strategies anticipated for the development of novel Cu-free catalyst systems with high C_{2+} product selectivity from a limited number of published examples. Benefit from the fast development of artificial intelligence, researchers can get more valuable guidance from the large number of results based on machine learning and DFT calculation. These calculated results can help researchers screen effective tandem sites to design Cu-free tandem catalysts to achieve electrocatalytic CO_2 to produce C_{2+} products. In addition, the microenvironment structure of the designed tandem catalysts is critical of the performance. Therefore, researchers should develop accurate synthetic methods to control the microenvironment structure at atom scale. In the future, it is expected to develop more efficient tandem catalysts to catalyze CRR to synthesize C_{2+} products, overcoming the disadvantages of Cu-based materials and promoting future commercial applications.

5 Conclusions and perspectives

In conclusion, tandem catalysts play a vital role in producing C_{2+} products via electrocatalytic CRR and tandem catalysis strategy is an effective route to enhance the C_{2+} performance of CRR. In this review, we systematically summarized the recent progress in tandem electrocatalysis for CO_2 reduction to prepare C_{2+} products (Table 1), including the origin and fundamental mechanism of tandem electrocatalysis, the strategies of catalyst design and regulation principles (Scheme 1). In addition, some newest findings that Cu-free tandem catalysts can achieve to produce C_{2+} products are well introduced. In each part, the tandem process and reaction mechanism are discussed in detail. Though there are so many great findings, several significant challenges still exist in this novel topic when considering the application. For the mechanism of electrocatalytic CO_2 reduction to prepare C_{2+} products via tandem catalysts, it still needs more fundamental research based on advanced experimental technologies and calculated models. And more *in-situ* or *operando* characterizations are expected to track the dynamic changes of both CO_2 molecule and tandem catalyst, which can assist to understand the real reaction process and mechanism. When considering the industrial application, the partial current density of C_{2+} products still cannot reach the requirement of industrial application. More attention is expected to focus on the

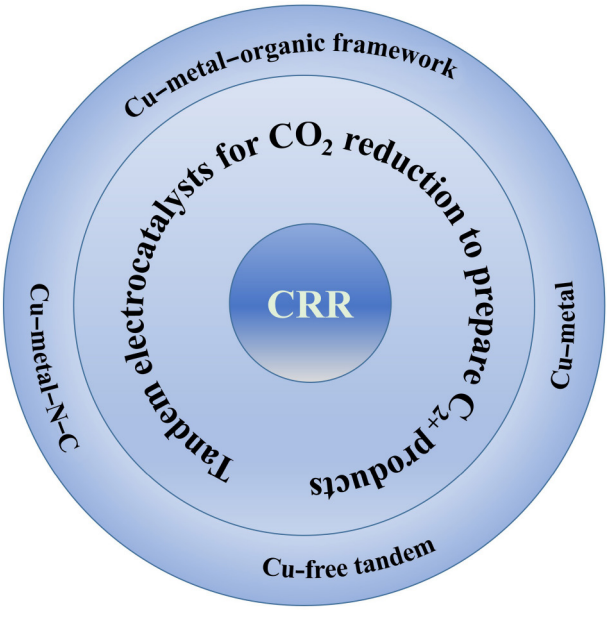

Scheme 1 Tandem electrocatalysts for CO_2 reduction to prepare multi-carbon products.

Table 1 Summary of recent key advances in tandem catalysts for electrocatalytic CO_2 reduction to produce C_{2+} products

Tandem catalysts	Product	FE (%)	Potential (V)	Current density (mA·cm^{-2})	Cell	Electrolyte	References
Cu-UiO-66	C_2H_4	44	−0.96 (RHE)	—	Flow cell	1 M KOH	[137]
MAF-2	C_2H_4	51.2	−1.3 (RHE)	12	H-cell	0.1 M $KHCO_3$	[138]
CuSn–HAB	C_2H_5OH	56	−0.57 (RHE)	68	Flow cell	1 M KOH	[135]
Cu-MOF	C_2H_4	11.30	−0.94 (RHE)	12.1	H-cell	0.5 M $KHCO_3$	[133]
Cu/Co SAC	C_{2+}	82	—	800	Flow cell	0.5 M H_3PO_4 + KH_2PO_4	[67]
Cu/Ni SAC	C_2H_4	62	−1.4 (RHE)	370	Flow cell	1 M $KHCO_3$	[123]
$AgIO_3$	C_{2+}	82.0	—	984	Flow cell	0.5 M K_2SO_4	[101]
Ag-Cu	C_{2+}	94	−0.65 (RHE)	720	Flow cell	1 M KOH	[94]
Cu-X-Cu	C_2H_5OH C_2H_4	32.69 36.54	−1.1 (RHE)	180	Flow cell	3 M KOH	[79]
BIT-119	C_2H_5OH C_2H_4	42.0 33.0	−1.8 (Ag/AgCl)	17	H-cell	1.0 M $KHCO_3$	[73]
SnS_2/Sn_1-O3G	C_2H_5OH	82.5	−0.9 (RHE)	17.8	H-cell	0.5 M Na_2SO_4	[69]

optimization of the electrolyser to avoid the limitation of the solubility of CO_2 in the electrolyte and enhance the current density. In addition, it is also very important to develop effective methods which can prepare the efficient tandem catalysts at a large scale with suitable costs. Most of the existing tandem catalysts were synthesized at the level of gram, it may face various challenges when magnifying the scale. Therefore, researchers should also develop potential methods which can synthesize the tandem catalysts at large scale with low cost and uniform properties. Apart from the Cu-based tandem catalysts, there are very few examples of Cu-free tandem catalysts for C_{2+} products. Therefore, it is suggested to combine machine learning and abundant calculated and experimental studies to develop ideal Cu-free tandem catalysts. In addition to activity and selectivity, researchers pay less attention to long-term stability of tandem catalysts. The stability performance is still far away from the requirement of industrial application. For the Cu-based tandem catalysts, the active sites may change or be lost during long-term operation, especially at the condition of large current density. Various strategies are expected to protect or regenerate the active sites to keep the performance for a long time. More researchers are expected to further focus on this novel field and promote its commercial applications.

Data availability

Not applicable.

Acknowledgements

This work is supported by National Natural Science Foundation of China (Nos. 22202065 and 22409159), Natural Science Foundation of Hubei Province of China (No. 2024AFB1004). Natural Science Basic Research Program of Shaanxi (Nos. 2024JC-YBQN-0119 and 2023SYJ04). We gratefully acknowledge the financial support from CHN Energy Zhejiang Ninghai Power Generation CO. Ltd. (No. GJNY-23-122).

Declaration of competing interest

All the contributing authors report no conflict of interests in this work.

Author contribution statement

Z. M. C.: Writing – original draft. X. W. S.: Investigation, writing – original draft. T. L.: Formal analysis. Y. G. Y.: Visualization. F. L.: Formal analysis. J. M.: Formal analysis. S. P. P.: Investigation. Z. W. T.: Formal analysis. F. K. F.: Writing – original draft. R. F. Y.: Writing – original draft. D. F. Y.: Writing – review & editing, supervision, funding acquisition. S. H. C.: Review & editing, supervision, funding acquisition. All the authors have approved the final manuscript.

Use of AI statement

None.

References

[1] Allen, M. R.; Frame, D. J.; Huntingford, C.; Jones, C. D.; Lowe, J. A.; Meinshausen, M.; Meinshausen, N. Warming caused by cumulative carbon emissions towards the trillionth tonne. *Nature* **2009**, *458*, 1163–1166.

[2] Hulme, M. 1.5 °C and climate research after the Paris agreement. *Nat. Climate Change* **2016**, *6*, 222–224.

[3] Teng, X.; Si, D.; Chen, L. S.; Shi, J. L. Synergetic catalytic effects by strong metal-support interaction for efficient electrocatalysis. *eScience* **2024**, *4*, 100272.

[4] Chen, Y. J.; Ji, S. F.; Chen, C.; Peng, Q.; Wang, D. S.; Li, Y. D. Single-atom catalysts: Synthetic strategies and electrochemical applications. *Joule* **2018**, *2*, 1242–1264.

[5] Wang, Y.; Zheng, X. B.; Wang, D. S. Design concept for electrocatalysts. *Nano Res.* **2022**, *15*, 1730–1752.

[6] Fang, W. S.; Guo, W.; Lu, R. H.; Yan, Y.; Liu, X. K.; Wu, D.; Li, F. M.; Zhou, Y. S.; He, C. H.; Xia, C. F. et al. Durable CO_2 conversion in the proton-exchange membrane system. *Nature* **2024**, *626*, 86–91.

[7] Wang, Y.; Ge, H. Y.; Luo, Y. X.; Zhu, X. J.; Wang, L. L.; Yan, D. F. Pulsed electrocatalysis: A dynamical route for tailoring electrocatalytic properties from fundamentals to applications. *Chem. Eng. J.* **2024**, *502*, 157783.

[8] Gao, W. Q.; Wang, C.; Lv, L.; Yan, D. F.; Xia, B. Y. Electrocatalytic bipolar synthesis of valuable chemicals. *ChemCatChem* **2024**, *16*, e202401198.

[9] Sun, H. X.; Gao, Y. Y.; Chen, M. Y.; Li, M.; Xia, Q. Q.; Liu, Y. Z.; Meng, J.; Dou, S.; Yu, H. P. Synergistic boosting the electrooxidation of biomass-based 5-hydroxymethylfurfural on cellulose-derived Co_3O_4/N-doped carbon catalysts. *Mater. Today Catal.* **2024**, *7*, 100062.

[10] Yan, D. F.; Mebrahtu, C.; Wang, S. Y.; Palkovits, R. Innovative electrochemical strategies for hydrogen production: From electricity input to electricity output. *Angew. Chem., Int. Ed.* **2023**, *62*, e202214333.

[11] Li, Y. P.; Niu, S. W.; Liu, P. G.; Pan, R. R.; Zhang, H. K.; Ahmad, N.; Shi, Y.; Liang, X.; Cheng, M. Y.; Chen, S. H. et al. Ruthenium nanoclusters and single atoms on α-MoC/N-doped carbon achieves low-input/input-free hydrogen evolution via decoupled/coupled hydrazine oxidation. *Angew. Chem.* **2024**, *136*, e202316755.

[12] Zheng, X. B.; Yang, J. R.; Li, P.; Jiang, Z. L.; Zhu, P.; Wang, Q. S.; Wu, J. B.; Zhang, E. H.; Sun, W. P.; Dou, S. X. et al. Dual-atom support boosts nickel-catalyzed urea electrooxidation. *Angew. Chem.* **2023**, *135*, e202217449.

[13] Zhong, Y.; Xiong, H. L.; Low, J.; Long, R.; Xiong, Y. J. Recent progress in electrochemical C–N coupling reactions. *eScience* **2023**, *3*, 100086.

[14] Lv, J. J.; Yin, R. N.; Zhou, L. M.; Li, J.; Kikas, R.; Xu, T.; Wang, Z. J.; Jin, H. L.; Wang, X.; Wang, S. Microenvironment engineering for the electrocatalytic CO_2 reduction reaction. *Angew. Chem.* **2022**, *134*, e202207252.

[15] Zhang, W.; Yang, Y.; Li, Y. X.; Li, F. W.; Luo, M. C. Recent progress on integrated CO_2 capture and electrochemical upgrading. *Mater. Today Catal.* **2023**, *2*, 100006.

[16] Ahmad, T.; Liu, S.; Sajid, M.; Li, K.; Ali, M.; Liu, L.; Chen, W. Electrochemical CO_2 reduction to C_{2+} products using Cu-based electrocatalysts: A review. *Nano Res. Energy* **2022**, *1*, 9120021.

[17] He, X. R.; Chen, J. W.; Xu, Y. F.; Shen, Y.; Zeng, Y. F.; Zhu, J. Y.; Xu, B. J.; Wang, C. Metal–organic layers induce *in situ* nano-structuring of Cu surface in electrocatalytic CO_2 reduction. *Nano Res.* **2023**, *16*, 4554–4561.

[18] Wang, S. W.; Wang, L. G.; Zhou, X. D.; Fang, J. J.; Deng, C.; Wang, D. S. Design principles of single-atom catalysts anchored over porous materials for green catalysis and conversion. *Nano Res.*, in press, DOI: 10.26599/NR.2025.94907137.

[19] Yang, J. R.; Zhu, C. X.; Li, W. H.; Zheng, X. S.; Wang, D. S. Organocatalyst supported by a single-atom support accelerates both electrodes used in the chlor-alkali industry via modification of non-covalent interactions. *Angew. Chem., Int. Ed.* **2024**, *63*, e202314382.

[20] Wang, X. Y.; Pan, Y. Z.; Yang, J. R.; Li, W. H.; Gan, T.; Pan, Y. M.; Tang, H. T.; Wang, D. S. Single-atom iron catalyst as an advanced redox mediator for anodic oxidation of organic electrosynthesis.

Angew. Chem., Int. Ed. **2024**, *63*, e202404295.
[21] Liu, Y. L.; Zhuang, Z. C.; Liu, Y. X.; Liu, N. Y.; Li, Y. X.; Cheng, Y. Y.; Yu, J. W.; Yu, R. H.; Wang, D. S.; Li, H. T. Shear-strained Pd single-atom electrocatalysts for nitrate reduction to ammonia. *Angew. Chem., Int. Ed.* **2024**, *63*, e202411396.
[22] Wang, C.; Gao, W. Q.; Hu, W.; Wen, W.; Wang, S. F.; Zhang, X. H.; Yan, D. F.; Xia, B. Y. Recent advances in electrochemical synthesis of urea via C–N coupling. *J. Energy Chem.* **2024**, *98*, 294–310.
[23] She, X. J.; Wang, Y. F.; Xu, H.; Chi Edman Tsang, S.; Ping Lau, S. Challenges and opportunities in electrocatalytic CO_2 reduction to chemicals and fuels. *Angew. Chem., Int. Ed.* **2022**, *61*, e202211396.
[24] Yang, P. P.; Gao, M. R. Enrichment of reactants and intermediates for electrocatalytic CO_2 reduction. *Chem. Soc. Rev.* **2023**, *52*, 4343–4380.
[25] Zhang, J. F.; Li, Z. Y.; Cai, R.; Zhang, T. Y.; Yang, S. Z.; Ma, L.; Wang, Y.; Wu, Y. C.; Wu, J. J. Switching CO_2 electroreduction selectivity between C_1 and C_2 hydrocarbons on Cu gas-diffusion electrodes. *Energy Environ. Mater.* **2023**, *6*, e12307.
[26] Zhang, B. K.; Jiang, J. W. $Mo_2B_2O_2$ MB ene for efficient electrochemical CO reduction to C_2 chemicals: Computational exploration. *Energy Enviro. Mater.* **2024**, *7*, e12738.
[27] Zhai, Y. J.; Han, P.; Yun, Q. B.; Ge, Y. Y.; Zhang, X.; Chen, Y.; Zhang, H. Phase engineering of metal nanocatalysts for electrochemical CO_2 reduction. *eScience* **2022**, *2*, 467–485.
[28] Chen, F. R.; Yao, Z. C.; Lyu, Z. H.; Fu, J. J.; Zhang, X. L.; Hu, J. S. Recent advances in p-block metal chalcogenide electrocatalysts for high-efficiency CO_2 reduction. *eScience* **2024**, *4*, 100172.
[29] Zhao, J.; Zhang, Y. X.; Zhuang, Z. C.; Deng, Y. T.; Gao, G.; Li, J. Y.; Meng, A. L.; Li, G. C.; Wang, L.; Li, Z. J. et al. Tailoring d–p orbital hybridization to decipher the essential effects of heteroatom substitution on redox kinetics. *Angew. Chem., Int. Ed.* **2024**, *63*, e202404968.
[30] Zhang, Y. D.; Sun, Y. J.; Wang, Q. Y.; Zhuang, Z. C.; Ma, Z. T.; Liu, L. M.; Wang, G. M.; Wang, D. S.; Zheng, X. S. Synergy of photogenerated electrons and holes toward efficient photocatalytic urea synthesis from CO_2 and N_2. *Angew. Chem., Int. Ed.* **2024**, *63*, e202405637.
[31] Zhang, M.; Lu, M.; Yang, M. Y.; Liao, J. P.; Liu, Y. F.; Yan, H. J.; Chang, J. N.; Yu, T. Y.; Li, S. L.; Lan, Y. Q. Ultrafine Cu nanoclusters confined within covalent organic frameworks for efficient electroreduction of CO_2 to CH_4 by synergistic strategy. *eScience* **2023**, *3*, 100116.
[32] Wang, F. S.; Ji, H. C.; Wu, Z. F.; Chen, K.; Gao, W. Q.; Wang, C.; Wang, L. L.; Chen, J. M.; Yan, D. F. The advanced development of one-dimensional transition metal dichalcogenide nanotubes: From preparation to application. *Chin. Chem. Lett.*, in press, DOI: 10.1016/j.cclet.2024.109898.
[33] Wang, S.; Zhang, J. L.; Yao, L.; Yang, Y. S.; Zheng, L. R.; Guan, B.; Zhao, Y. Z.; Wang, Y. Y.; Han, B. X.; Xing, X. Q. Efficient electrocatalytic CO_2 reduction to C_{2+} chemicals on internal porous copper. *Nano Res.* **2023**, *16*, 10779–10786.
[34] Gu, Z. X.; Shen, H.; Chen, Z.; Yang, Y. Y.; Yang, C.; Ji, Y. L.; Wang, Y. H.; Zhu, C.; Liu, J. L.; Li, J. et al. Efficient electrocatalytic CO_2 reduction to C_{2+} alcohols at defect-site-rich Cu surface. *Joule* **2021**, *5*, 429–440.
[35] Xia, J. K.; Xu, J. W.; Yu, B.; Liang, X.; Qiu, Z.; Li, H.; Feng, H. J.; Li, Y. F.; Cai, Y. J.; Wei, H. Y. et al. A metal-sulfur-carbon catalyst mimicking the two-component architecture of nitrogenase. *Angew. Chem.* **2024**, *136*, e202412740.
[36] Wang, X. D.; Hu, Q.; Li, G. D.; Yang, H. P.; He, C. X. Recent advances and perspectives of electrochemical CO_2 reduction toward C_{2+} products on Cu-based catalysts. *Electrochem. Energy Rev.* **2022**, *5*, 28.
[37] Xu, C. C.; Zhi, X.; Vasileff, A.; Wang, D.; Jin, B.; Jiao, Y.; Zheng, Y.; Qiao, S. Z. Highly selective two-electron electrocatalytic CO_2 reduction on single-atom Cu catalysts. *Small Struct.* **2021**, *2*, 2000058.
[38] Larrazábal, G. O.; Martín, A. J.; Mitchell, S.; Hauert, R.; Pérez-Ramírez, J. Enhanced reduction of CO_2 to CO over Cu–In electrocatalysts: Catalyst evolution is the key. *ACS Catal.* **2016**, *6*, 6265–6274.
[39] Ren, W. H.; Tan, X.; Qu, J. T.; Li, S. S.; Li, J. T.; Liu, X.; Ringer, S. P.; Cairney, J. M.; Wang, K. X.; Smith, S. C. et al. Isolated copper–tin atomic interfaces tuning electrocatalytic CO_2 conversion. *Nat. Commun.* **2021**, *12*, 1449.
[40] Chen, Y.; Fan, Z. X.; Wang, J.; Ling, C. Y.; Niu, W. X.; Huang, Z. Q.; Liu, G. G.; Chen, B.; Lai, Z. C.; Liu, X. Z. et al. Ethylene selectivity in electrocatalytic CO_2 reduction on Cu nanomaterials: A crystal phase-dependent study. *J. Am. Chem. Soc.* **2020**, *142*, 12760–12766.
[41] Zhang, T. T.; Yuan, B. W.; Wang, W. L.; He, J.; Xiang, X. Tailoring *H intermediate coverage on the $CuAl_2O_4$/CuO catalyst for enhanced electrocatalytic CO_2 reduction to ethanol. *Angew. Chem.* **2023**, *135*, e202302096.
[42] Wang, D.; Mao, J. J.; Zhang, C. C.; Zhang, J. W.; Li, J. S.; Zhang, Y.; Zhu, Y. F. Modulating microenvironments to enhance CO_2 electroreduction performance. *eScience* **2023**, *3*, 100119.
[43] Zeng, M.; Fang, W. S.; Cen, Y. R.; Zhang, X. Y.; Hu, Y. M.; Xia, B. Y. Reaction environment regulation for electrocatalytic CO_2 reduction in acids. *Angew. Chem.* **2024**, *136*, e202404574.
[44] Yan, D. F.; Li, Y. X.; Huo, J.; Chen, R.; Dai, L. M.; Wang, S. Y. Defect chemistry of nonprecious-metal electrocatalysts for oxygen reactions. *Adv. Mater.* **2017**, *29*, 1606459.
[45] Yan, D. F.; Xia, C. F.; Zhang, W. J.; Hu, Q.; He, C. X.; Xia, B. Y.; Wang, S. Y. Cation defect engineering of transition metal electrocatalysts for oxygen evolution reaction. *Adv. Energy Mater.* **2022**, *12*, 2202317.
[46] Wang, Y. F.; Han, P.; Lv, X. M.; Zhang, L. J.; Zheng, G. F. Defect and interface engineering for aqueous electrocatalytic CO_2 reduction. *Joule* **2018**, *2*, 2551–2582.
[47] Pan, F. P.; Yang, Y. Designing CO_2 reduction electrode materials by morphology and interface engineering. *Energy Environ. Sci.* **2020**, *13*, 2275–2309.
[48] Zang, D. J.; Gao, X. J.; Li, L. Y.; Wei, Y. G.; Wang, H. Q. Confined interface engineering of self-supported Cu@N-doped graphene for electrocatalytic CO_2 reduction with enhanced selectivity towards ethanol. *Nano Res.* **2022**, *15*, 8872–8879.
[49] Vasileff, A.; Xu, C. C.; Jiao, Y.; Zheng, Y.; Qiao, S. Z. Surface and interface engineering in copper-based bimetallic materials for selective CO_2 electroreduction. *Chem* **2018**, *4*, 1809–1831.
[50] Yang, Y.; Zhang, Y.; Hu, J. S.; Wan, L. J. Progress in the mechanisms and materials for CO_2 electroreduction toward C_{2+} products. *Acta Phys.-Chim. Sin.* **2020**, *36*, 1906085.
[51] Yan, T. X.; Chen, X. Y.; Kumari, L.; Lin, J. L.; Li, M. L.; Fan, Q.; Chi, H. Y.; Meyer, T. J.; Zhang, S.; Ma, X. B. Multiscale CO_2 electrocatalysis to C_{2+} products: Reaction mechanisms, catalyst design, and device fabrication. *Chem. Rev.* **2023**, *123*, 10530–10583.
[52] Zhang, L.; Zhao, Z. J.; Gong, J. L. Nanostructured materials for heterogeneous electrocatalytic CO_2 reduction and their related reaction mechanisms. *Angew. Chem., Int. Ed.* **2017**, *56*, 11326–11353.
[53] Zhu, Q. S.; Murphy, C. J.; Baker, L. R. Opportunities for electrocatalytic CO_2 reduction enabled by surface ligands. *J. Am. Chem. Soc.* **2022**, *144*, 2829–2840.
[54] Hu, Y.; Asif, M.; Gong, J. X.; Zeb, H.; Lan, H. H.; Kashif Khan, M.; Xia, H. C.; Du, M. L. Mechanistic insights into C–C coupling in electrocatalytic CO_2 reduction reaction. *Chem. Commun.* **2024**, *60*, 10618–10628.
[55] Chen, C. B.; Yu, S.; Yang, Y.; Louisia, S.; Roh, I.; Jin, J. B.; Chen, S. P.; Chen, P. C.; Shan, Y.; Yang, P. D. Exploration of the bio-analogous asymmetric C–C coupling mechanism in tandem CO_2 electroreduction. *Nat. Catal.* **2022**, *5*, 878–887.
[56] Li, H. B.; Li, X. Y.; Wang, P. T.; Zhang, Z.; Davey, K.; Shi, J. Q.;

Qiao, S. Z. Machine learning big data set analysis reveals C–C electro-coupling mechanism. *J. Am. Chem. Soc.* **2024**, *146*, 22850–22858.

[57] Zhang, M. Y.; Zhou, D. Y.; Mu, X. Q.; Wang, D. S.; Liu, S.; Dai, Z. H. Regulating the critical intermediates of dual-atom catalysts for CO_2 electroreduction. *Small* **2024**, *20*, 2402050.

[58] Zheng, M.; Wang, P. T.; Zhi, X.; Yang, K.; Jiao, Y.; Duan, J. J.; Zheng, Y.; Qiao, S. Z. Electrocatalytic CO_2-to-C_{2+} with ampere-level current on heteroatom-engineered copper via tuning *CO intermediate coverage. *J. Am. Chem. Soc.* **2022**, *144*, 14936–14944.

[59] Li, J.; Wang, Z. Y.; McCallum, C.; Xu, Y.; Li, F. W.; Wang, Y. H.; Gabardo, C. M.; Dinh, C. T.; Zhuang, T. T.; Wang, L. et al. Constraining CO coverage on copper promotes high-efficiency ethylene electroproduction. *Nat. Catal.* **2019**, *2*, 1124–1131.

[60] Sun, Q.; Tan, X.; Jia, C.; Rong, C. L.; Wang, S. H.; Han, C.; Xiao, Y.; Qi, H. Q.; Smith, S. C.; Zhao, C. Molecule doping of atomically dispersed Cu–Au alloy for enhancing electroreduction of CO to C_{2+} products. *Adv. Funct. Mater.* **2024**, *34*, 2406281.

[61] Rhimi, B.; Zhou, M.; Yan, Z. X.; Cai, X. Y.; Jiang, Z. F. Cu-based materials for enhanced C_{2+} product selectivity in photo-/electro-catalytic CO_2 reduction: Challenges and prospects. *Nano-Micro Lett.* **2024**, *16*, 64.

[62] Lin, Y. R.; Lee, D. U.; Tan, S. Q.; Koshy, D. M.; Lin, T. Y.; Wang, L.; Corral, D.; Avilés Acosta, J. E.; Zamora Zeledon, J. A.; Beck, V. A. et al. Vapor-fed electrolyzers for carbon dioxide reduction using tandem electrocatalysts: Cuprous oxide coupled with nickel-coordinated nitrogen-doped carbon. *Adv. Funct. Mater.* **2022**, *32*, 2113252.

[63] Xie, G. X.; Guo, W. W.; Fang, Z. J.; Duan, Z. X.; Lang, X. Z.; Liu, D. D.; Mei, G. L.; Zhai, Y. L.; Sun, X. F.; Lu, X. Q. Dual-metal sites drive tandem electrocatalytic CO_2 to C_{2+} products. *Angew. Chem., Int. Ed.* **2024**, *63*, e202412568.

[64] Luan, P.; Dong, X.; Liu, L. Q.; Xiao, J. P.; Zhang, P. F.; Zhang, J.; Chi, H. B.; Wang, Q. N.; Ding, C. M.; Li, R. G. et al. Selective electrosynthesis of ethanol via asymmetric C–C coupling in tandem CO_2 reduction. *ACS Catal.* **2024**, *14*, 8776–8785.

[65] Duan, G. Y.; Li, X. Q.; Ding, G. R.; Han, L. J.; Xu, B. H.; Zhang, S. J. Highly efficient electrocatalytic CO_2 reduction to C_{2+} products on a poly (ionic liquid)-based Cu^0–Cu^I tandem catalyst. *Angew. Chem.* **2022**, *134*, e202110657.

[66] Zhang, B.; Wang, L. L.; Li, D.; Li, Z. M.; Bu, R.; Lu, Y. Y. Tandem strategy for electrochemical CO_2 reduction reaction. *Chem Catal.* **2022**, *2*, 3395–3429.

[67] Chen, Y. J.; Li, X. Y.; Chen, Z.; Ozden, A.; Huang, J. E.; Ou, P. F.; Dong, J. C.; Zhang, J. Q.; Tian, C.; Lee, B. H. et al. Efficient multicarbon formation in acidic CO_2 reduction via tandem electrocatalysis. *Nat. Nanotechnol.* **2024**, *19*, 311–318.

[68] Chen, S. H.; Zheng, X. B.; Zhu, P.; Li, Y. P.; Zhuang, Z. C.; Wu, H. J.; Zhu, J. X.; Xiao, C. H.; Chen, M. Z.; Wang, P. S. et al. Copper atom pairs stabilize *OCCO dipole toward highly selective CO_2 electroreduction to C_2H_4. *Angew. Chem., Int. Ed.* **2024**, *63*, e202411591.

[69] Ding, J.; Bin Yang, H.; Ma, X. L.; Liu, S.; Liu, W.; Mao, Q.; Huang, Y. Q.; Li, J.; Zhang, T.; Liu, B. A tin-based tandem electrocatalyst for CO_2 reduction to ethanol with 80% selectivity. *Nat. Energy* **2023**, *8*, 1386–1394.

[70] Li, J.; Chen, G. X.; Zhu, Y. Y.; Liang, Z.; Pei, A.; Wu, C. L.; Wang, H. X.; Lee, H. R.; Liu, K.; Chu, S. et al. Efficient electrocatalytic CO_2 reduction on a three-phase interface. *Nat. Catal.* **2018**, *1*, 592–600.

[71] Qin, Y. Y.; Zhao, W. S.; Xia, C. F.; Yu, L. J.; Song, F.; Zhang, J. R.; Wu, T. T.; Cao, R.; Ding, S. J.; Xia, B. Y. et al. CO intermediate-assisted dynamic cu sintering during electrocatalytic CO_2 reduction on Cu–N–C catalysts. *Angew. Chem., Int. Ed.* **2024**, *63*, e202404763.

[72] Bai, H. P.; Cheng, T.; Li, S. Y.; Zhou, Z. Y.; Yang, H.; Li, J.; Xie, M.; Ye, J. Y.; Ji, Y. J.; Li, Y. Y. et al. Controllable CO adsorption determines ethylene and methane productions from CO_2 electroreduction. *Sci. Bull.* **2021**, *66*, 62–68.

[73] Wang, C. L.; Lv, Z. H.; Liu, Y. R.; Dai, L.; Liu, R.; Sun, C. T.; Liu, W. Y.; Feng, X.; Yang, W. X.; Wang, B. Asymmetric Cu–N_1O_3 sites coupling atop-type and bridge-type adsorbed *C_1 for electrocatalytic CO_2-to-C_2 conversion. *Angew. Chem., Int. Ed.* **2024**, *63*, e202411216.

[74] Chen, C. J.; Huang, L. S.; Jiang, Y. L.; Zheng, Y.; Qiao, S. Z. Modulating local environment for electrocatalytic CO_2 reduction to alcohol. *Nano Energy* **2024**, *126*, 109656.

[75] Wang, X. L.; de Araújo, J. F.; Ju, W.; Bagger, A.; Schmies, H.; Kühl, S.; Rossmeisl, J.; Strasser, P. Mechanistic reaction pathways of enhanced ethylene yields during electroreduction of CO_2–CO co-feeds on Cu and Cu-tandem electrocatalysts. *Nat. Nanotechnol.* **2019**, *14*, 1063–1070.

[76] Yang, Y. S.; Zhang, J. L.; Tan, Z. H.; Yang, J.; Wang, S.; Li, M. L.; Su, Z. Z. Highly selective production of C_{2+} oxygenates from CO_2 in strongly acidic condition by rough Ag–Cu electrocatalyst. *Angew. Chem., Int. Ed.* **2024**, *63*, e202408873.

[77] Jiang, K.; Cai, W. B. Disentangling distinct Cu surface sites for electrocatalytic CO_2-to-CO and CO-to-C_{2+} conversion. *Sci. China Chem.* **2024**, *67*, 1047–1048.

[78] Guan, S. Y.; Yuan, Z. L.; Zhao, S. Q.; Zhuang, Z. C.; Zhang, H. H.; Shen, R. F.; Fan, Y. P.; Li, B. J.; Wang, D. S.; Liu, B. Z. Efficient hydrogen generation from ammonia borane hydrolysis on a tandem ruthenium-platinum-titanium catalyst. *Angew. Chem., Int. Ed.* **2024**, *63*, e202408193.

[79] Ma, F. Y.; Zhang, P. F.; Zheng, X. B.; Chen, L.; Li, Y. R.; Zhuang, Z. C.; Fan, Y. M.; Jiang, P.; Zhao, H.; Zhang, J. W. et al. Steering the site distance of atomic Cu–Cu pairs by first-shell halogen coordination boosts CO_2-to-C_2 selectivity. *Angew. Chem., Int. Ed.* **2024**, *63*, e202412785.

[80] Tang, M. H.; Shen, J.; Zhang, F. T.; Zhao, Y. F.; Gan, T.; Zeng, W.; Li, R. X.; Wang, D. S.; Han, B. X.; Liu, Z. M. Upcycling of polyamide wastes to tertiary amines using Mo single atoms and Rh nanoparticles. *Angew. Chem.*, in press, DOI: 10.1002/ange.202416436.

[81] Zhan, C.; Dattila, F.; Rettenmaier, C.; Bergmann, A.; Kühl, S.; García-Muelas, R.; López, N.; Cuenya, B. R. Revealing the CO coverage-driven C–C coupling mechanism for electrochemical CO_2 reduction on Cu_2O nanocubes via *operando* Raman spectroscopy. *ACS Catal.* **2021**, *11*, 7694–7701.

[82] Chang, X. X.; Xiong, H. C.; Lu, Q.; Xu, B. J. Mechanistic implications of low CO coverage on Cu in the electrochemical CO and CO_2 reduction reactions. *JACS Au* **2023**, *3*, 2948–2963.

[83] Wang, Y.; Wang, J. R.; Cai, R.; Zhang, J. F.; Xia, S.; Li, Z. P.; Yu, C. P.; Wu, J. J.; Wang, P.; Wu, Y. C. Enhanced local CO coverage on Cu quantum dots for boosting electrocatalytic CO_2 reduction to ethylene. *Adv. Funct. Mater.*, in press, DOI: 10.1002/adfm.202417764.

[84] Wang, M.; Nikolaou, V.; Loiudice, A.; Sharp, I. D.; Llobet, A.; Buonsanti, R. Tandem electrocatalytic CO_2 reduction with Fe-porphyrins and Cu nanocubes enhances ethylene production. *Chem. Sci.* **2022**, *13*, 12673–12680.

[85] Xu, W. J.; Shang, H. S.; Guan, J.; Yang, X. Y.; Jin, X. Y.; Tao, L. M.; Shao, Z. Q. Research progress of dual-site tandem catalysts in the preparation of multi carbon products by electro reduction of CO_2. *Adv. Funct. Mater.* **2025**, *35*, 2412812.

[86] Kim, Y. E.; Park, J. E.; Lee, J. H.; Choi, H.; Lee, W.; Ko, Y. N.; Kim, H. Y.; Park, K. T. Ag decorated-Cu_2O catalysts with enhanced selectivity for CO_2 electroreduction toward C_{2+} products. *J. Environ. Chem. Eng.* **2023**, *11*, 111028.

[87] Fang, Z. J.; Guo, W. W.; Xie, G. X.; Mei, G. L.; Zhai, Y. L.; Zhu, Z. J.; Lu, X. Q.; Tang, J. G. Enhanced CO_2 electroreduction to C_{2+} production on asymmetric Zn–O–Cu sites via tuning of *CO intermediate adsorption. *Appl. Catal. B: Environ. Energy* **2024**, *359*, 124473.

[88] Morales-Guio, C. G.; Cave, E. R.; Nitopi, S. A.; Feaster, J. T.; Wang, L.; Kuhl, K. P.; Jackson, A.; Johnson, N. C.; Abram, D. N.; Hatsukade, T. et al. Improved CO_2 reduction activity towards C_{2+} alcohols on a tandem gold on copper electrocatalyst. *Nat. Catal.* **2018**, *1*, 764–771.

[89] Gao, J.; Zhang, H.; Guo, X. Y.; Luo, J. S.; Zakeeruddin, S. M.; Ren, D.; Grätzel, M. Selective C–C coupling in carbon dioxide electroreduction via efficient spillover of intermediates as supported by *operando* Raman spectroscopy. *J. Am. Chem. Soc.* **2019**, *141*, 18704–18714.

[90] Song, J. T.; Qian, Z. X.; Yang, J.; Lin, X. M.; Xu, Q. C.; Li, J. F. *In situ*/*operando* investigation for heterogeneous electro-catalysts: From model catalysts to state-of-the-art catalysts. *ACS Energy Lett.* **2024**, *9*, 4414–4440.

[91] Yang, Y.; Louisia, S.; Yu, S.; Jin, J. B.; Roh, I.; Chen, C. B.; Fonseca Guzman, M. V.; Feijóo, J.; Chen, P. C.; Wang, H. S. et al. *Operando* studies reveal active Cu nanograins for CO_2 electroreduction. *Nature* **2023**, *614*, 262–269.

[92] Cao, X. Y.; Tan, D. X.; Wulan, B.; Hui, K. S.; Hui, K. N.; Zhang, J. T. *In situ* characterization for boosting electrocatalytic carbon dioxide reduction. *Small Methods* **2021**, *5*, 2100700.

[93] Wang, Y.; Ma, F. Y.; Zhang, G. Q.; Zhang, J. W.; Zhao, H.; Dong, Y. M.; Wang, D. S. Precise synthesis of dual atom sites for electrocatalysis. *Nano Res.* **2024**, *17*, 9397–9427.

[94] Du, C.; Mills, J. P.; Yohannes, A. G.; Wei, W.; Wang, L.; Lu, S. Y.; Lian, J. X.; Wang, M. Y.; Guo, T.; Wang, X. Y. et al. Cascade electrocatalysis via AgCu single-atom alloy and Ag nanoparticles in CO_2 electroreduction toward multicarbon products. *Nat. Commun.* **2023**, *14*, 6142.

[95] Ning, S. B.; Ou, H. H.; Li, Y. G.; Lv, C. C.; Wang, S. F.; Wang, D. S.; Ye, J. H. Co^0–$Co^{\delta+}$ interface double-site-mediated C–C coupling for the photothermal conversion of CO_2 into light olefins. *Angew. Chem., Int. Ed.* **2023**, *62*, e202302253.

[96] Kong, X. D.; Zhao, J. K.; Ke, J. W.; Wang, C.; Li, S. J.; Si, R.; Liu, B.; Zeng, J.; Geng, Z. G. Understanding the effect of *CO coverage on C–C coupling toward CO_2 electroreduction. *Nano Lett.* **2022**, *22*, 3801–3808.

[97] Kibria, M. G.; Dinh, C. T.; Seifitokaldani, A.; De Luna, P.; Burdyny, T.; Quintero-Bermudez, R.; Ross, M. B.; Bushuyev, O. S.; García de Arquer, F. P.; Yang, P. D. et al. A surface reconstruction route to high productivity and selectivity in CO_2 electroreduction toward C_{2+} hydrocarbons. *Adv. Mater.* **2018**, *30*, 1804867.

[98] Jiang, Y. W.; Wang, X. Y.; Duan, D. L.; He, C. H.; Ma, J.; Zhang, W. Q.; Liu, H. J.; Long, R.; Li, Z. B.; Kong, T. T. et al. Structural reconstruction of Cu_2O superparticles toward electrocatalytic CO_2 reduction with high C_{2+} products selectivity. *Adv. Sci.* **2022**, *9*, 2105292.

[99] He, C. H.; Duan, D. L.; Low, J.; Bai, Y.; Jiang, Y. W.; Wang, X. Y.; Chen, S. M.; Long, R.; Song, L.; Xiong, Y. J. $Cu_{2-x}S$ derived copper nanoparticles: A platform for unraveling the role of surface reconstruction in efficient electrocatalytic CO_2-to-C_2H_4 conversion. *Nano Res.* **2023**, *16*, 4494–4498.

[100] Gao, X. Y.; Jiang, Y. J.; Liu, J. Y.; Shi, G. S.; Yang, C. L.; Xu, Q. S.; Yun, Y. Q.; Shen, Y. L.; Chang, M. W.; Zhu, C. Y. et al. Intermediate-regulated dynamic restructuring at Ag–Cu biphasic interface enables selective CO_2 electroreduction to C_{2+} fuels. *Nat. Commun.* **2024**, *15*, 10331.

[101] Yang, R. O.; Wen, Q. L.; Yang, Y. Q.; Liu, Y. W.; Yang, Y.; Wu, M.; Wei, Y.; Mei, B. B.; Liu, Y.; Li, H. Q. et al. Directional reconstruction to highly active tandem sites for superior acidic CO_2 electroreduction. *Adv. Mater.*, in press, DOI: 10.1002/adma.202414642.

[102] Chen, R. Z.; Chen, S. H.; Wang, L. Q.; Wang, D. S. Nanoscale metal particle modified single-atom catalyst: Synthesis, characterization, and application. *Adv. Mater.* **2024**, *36*, 2304713.

[103] Han, A. L.; Sun, W. M.; Wan, X.; Cai, D. D.; Wang, X. J.; Li, F.; Shui, J. L.; Wang, D. S. Construction of Co_4 atomic clusters to enable Fe–N_4 motifs with highly active and durable oxygen reduction performance. *Angew. Chem., Int. Ed.* **2023**, *62*, e202303185.

[104] Li, R. Z.; Zhao, J.; Liu, B. Z.; Wang, D. S. Atomic distance engineering in metal catalysts to regulate catalytic performance. *Adv. Mater.* **2024**, *36*, 2308653.

[105] Lin, L.; Su, P. Y.; Han, Y. T.; Xu, Y. M.; Ni, Q.; Zhang, X. Y.; Xiong, P. X.; Sun, Z. M.; Sun, G. B.; Chen, X. B. Advances in regulating the electron spin effect toward electrocatalysis applications. *eScience* **2025**, *5*, 100264.

[106] Mu, X. Q.; Liu, S. L.; Zhang, M. Y.; Zhuang, Z. C.; Chen, D.; Liao, Y. R.; Zhao, H. Y.; Mu, S. C.; Wang, D. S.; Dai, Z. H. Symmetry-broken Ru nanoparticles with parasitic Ru–Co dual-single atoms overcome the volmer step of alkaline hydrogen oxidation. *Angew. Chem.* **2024**, *136*, e202319618.

[107] Tao, Y.; Guan, J. P.; Zhang, J.; Hu, S. Y.; Ma, R. Z.; Zheng, H. R.; Gong, J. X.; Zhuang, Z. C.; Liu, S. J.; Ou, H. H. et al. Ruthenium single atomic sites surrounding the support pit with exceptional photocatalytic activity. *Angew. Chem., Int. Ed.* **2024**, *63*, e202400625.

[108] Zhuang, J. H.; Wang, D. S. Recent advances of single-atom alloy catalyst: Properties, synthetic methods and electrocatalytic applications. *Mater. Today Catal.* **2023**, *2*, 100009.

[109] Zhu, C. X.; Yang, J. R.; Zhang, J. W.; Wang, X. Q.; Gao, Y.; Wang, D. S.; Pan, H. G. Single-atom materials: The application in energy conversion. *Interdiscip. Mater.* **2024**, *3*, 74–86.

[110] Gan, T.; Wang, D. S. Atomically dispersed materials: Ideal catalysts in atomic era. *Nano Res.* **2024**, *17*, 18–38.

[111] Tang, Q. Q.; Feng, L. F.; Li, Z. P.; Wu, S. H.; Zhang, L. S.; Sun, Q.; Wu, M. F.; Zou, J. P. Single-atom sites regulation by the second-shell doping for efficient electrochemical CO_2 reduction. *Chin. Chem. Lett.* **2024**, *35*, 109454.

[112] Wong, H. H.; Sun, M. Z.; Wu, T.; Chan, C. H.; Lu, L.; Lu, Q. Y.; Chen, B. A.; Huang, B. L. Neighboring effect in single-atom catalysts for the electrochemical carbon dioxide reduction reaction. *eScience* **2024**, *4*, 100140.

[113] Xiong, J. X.; Ji, J. P.; Lei, Q.; Yang, X. C.; Bai, Y.; Zhang, X. L.; Cheng, H. M. Synergetic energy coupled thermal catalytic systems for CO_2 reduction. *eScience*, in press, DOI: 10.1016/j.esci.2024.100306.

[114] Wu, Y. S.; Liang, Y. Y.; Wang, H. L. Heterogeneous molecular catalysts of metal phthalocyanines for electrochemical CO_2 reduction reactions. *Acc. Chem. Res.* **2021**, *54*, 3149–3159.

[115] Jiang, Z.; Wang, Y.; Zhang, X.; Zheng, H. Z.; Wang, X. J.; Liang, Y. Y. Revealing the hidden performance of metal phthalocyanines for CO_2 reduction electrocatalysis by hybridization with carbon nanotubes. *Nano Res.* **2019**, *12*, 2330–2334.

[116] Chen, K. J.; Cao, M. Q.; Lin, Y. Y.; Fu, J. W.; Liao, H. X.; Zhou, Y. J.; Li, H. M.; Qiu, X. Q.; Hu, J. H.; Zheng, X. S. et al. Ligand engineering in nickel phthalocyanine to boost the electrocatalytic reduction of CO_2. *Adv. Funct. Mater.* **2022**, *32*, 2111322.

[117] Han, N.; Wang, Y.; Ma, L.; Wen, J. G.; Li, J.; Zheng, H. C.; Nie, K. Q.; Wang, X. X.; Zhao, F. P.; Li, Y. F. et al. Supported cobalt polyphthalocyanine for high-performance electrocatalytic CO_2 reduction. *Chem* **2017**, *3*, 652–664.

[118] Zheng, T. T.; Jiang, K.; Ta, N.; Hu, Y. F.; Zeng, J.; Liu, J. Y.; Wang, H. T. Large-scale and highly selective CO_2 electrocatalytic reduction on nickel single-atom catalyst. *Joule* **2019**, *3*, 265–278.

[119] Gong, Y. N.; Jiao, L.; Qian, Y. Y.; Pan, C. Y.; Zheng, L. R.; Cai, X. C.; Liu, B.; Yu, S. H.; Jiang, H. L. Regulating the coordination environment of MOF-templated single-atom nickel electrocatalysts for boosting CO_2 reduction. *Angew. Chem.* **2020**, *132*, 2727–2731.

[120] Gao, Y.; Liu, B. Z.; Wang, D. S. Microenvironment engineering of single/dual-atom catalysts for electrocatalytic application. *Adv. Mater.* **2023**, *35*, 2209654.

[121] Wang, X. L.; Ju, W.; Liang, L.; Riyaz, M.; Bagger, A.; Filippi, M.; Rossmeisl, J.; Strasser, P. Electrochemical CO_2 activation and

valorization on metallic copper and carbon-embedded N-coordinated single metal MNC catalysts. *Angew. Chem.* **2024**, *136*, e202401821.
[122] Yang, Q. H.; Liu, H.; Lin, Y. C.; Su, D. S.; Tang, Y. L.; Chen, L. Atomically dispersed metal catalysts for the conversion of CO_2 into high-value C_{2+} chemicals. *Adv. Mater.* **2024**, *36*, 2310912.
[123] Liu, M.; Wang, Q. Y.; Luo, T.; Herran, M.; Cao, X. Y.; Liao, W. R.; Zhu, L.; Li, H. M.; Stefancu, A.; Lu, Y. R. et al. Potential alignment in tandem catalysts enhances CO_2-to-C_2H_4 conversion efficiencies. *J. Am. Chem. Soc.* **2024**, *146*, 468–475.
[124] Xie, X. L.; Zhang, X.; Xie, M.; Xiong, L. K.; Sun, H.; Lu, Y. T.; Mu, Q. Q.; Rummeli, M. H.; Xu, J. B.; Li, S. et al. Au-activated N motifs in non-coherent cupric porphyrin metal–organic frameworks for promoting and stabilizing ethylene production. *Nat. Commun.* **2022**, *13*, 63.
[125] Chen, S. H.; Ye, C. L.; Wang, Z. W.; Li, P.; Jiang, W. J.; Zhuang, Z. C.; Zhu, J. X.; Zheng, X. B.; Zaman, S.; Ou, H. H. et al. Selective CO_2 reduction to ethylene mediated by adaptive small-molecule engineering of copper-based electrocatalysts. *Angew. Chem.* **2023**, *135*, e202315621.
[126] Liu, K. K.; Meng, Z.; Fang, Y.; Jiang, H. L. Conductive MOFs for electrocatalysis and electrochemical sensor. *eScience* **2023**, *3*, 100133.
[127] Zhu, Y. T.; Cui, X. Y.; Liu, H. L.; Guo, Z. G.; Dang, Y. F.; Fan, Z. X.; Zhang, Z. C.; Hu, W. P. Tandem catalysis in electrochemical CO_2 reduction reaction. *Nano Res.* **2021**, *14*, 4471–4486.
[128] Wen, C. F.; Zhou, M.; Liu, P. F.; Liu, Y. W.; Wu, X. F.; Mao, F. X.; Dai, S.; Xu, B. B.; Wang, X. L.; Jiang, Z. et al. Highly ethylene-selective electrocatalytic CO_2 reduction enabled by isolated Cu–S motifs in metal–organic framework based precatalysts. *Angew. Chem., Int. Ed.* **2022**, *61*, e202111700.
[129] Guan, H. X.; Zhang, Y. X.; Fan, W. J.; Yang, K.; Li, G.; Chen, S.; Li, L. Q.; Duan, J. J. Regulated Cu diatomic distance promoting carbon-carbon coupling during CO_2 electroreduction. *Small* **2024**, *21*, 2406605.
[130] Shao, B.; Huang, D.; Huang, R. K.; He, X. L.; Luo, Y.; Xiang, Y. L.; Jiang, L. B.; Dong, M.; Li, S. X.; Zhang, Z. et al. Metal–organic framework supported low-nuclearity cluster catalysts for highly selective carbon dioxide electroreduction to ethanol. *Angew. Chem., Int. Ed.* **2024**, *63*, e202409270.
[131] Li, Z. X.; Qiu, X. F.; Liao, P. Q. Efficient electroreduction of CO_2 to acetate with relative purity of 100% by ultrasmall Cu_2O nanoparticle on a conductive metal–organic framework. *Chin. Chem. Lett.*, in press, DOI: 10.1016/j.cclet.2024.110473.
[132] Huang, L.; Liu, Z. A.; Gao, G.; Chen, C. L.; Xue, Y. R.; Zhao, J. W.; Lei, Q.; Jin, M. T.; Zhu, C. Q.; Han, Y. et al. Enhanced CO_2 electroreduction selectivity toward ethylene on pyrazolate-stabilized asymmetric Ni–Cu hybrid sites. *J. Am. Chem. Soc.* **2023**, *145*, 26444–26451.
[133] Shao, P.; Zhou, W.; Hong, Q. L.; Yi, L. C.; Zheng, L. R.; Wang, W. J.; Zhang, H. X.; Zhang, H. B.; Zhang, J. Synthesis of a boron-imidazolate framework nanosheet with dimer copper units for CO_2 electroreduction to ethylene. *Angew. Chem., Int. Ed.* **2021**, *60*, 16687–16692.
[134] He, Q. Z.; Li, H. W.; Hu, Z. F.; Lei, L.; Wang, D. G.; Li, T. T. Highly selective CO_2 electroreduction to C_2H_4 using a dual-sites Cu(II) porphyrin framework coupled with Cu_2O nanoparticles via a synergetic-tandem strategy. *Angew. Chem., Int. Ed.* **2024**, *63*, e202407090.
[135] Zhao, Z. H.; Huang, J. R.; Liao, P. Q.; Chen, X. M. Highly efficient electroreduction of CO_2 to ethanol via asymmetric C–C Coupling by a metal–organic framework with heterodimetal dual sites. *J. Am. Chem. Soc.* **2023**, *145*, 26783–26790.
[136] Singh, A. K.; Gu, L.; Dutta Chowdhury, A.; Indra, A. Exploring ligand-controlled C_2 product selectivity in carbon dioxide reduction with copper metal–organic framework nanosheets. *Inorg. Chem.* **2023**, *62*, 8803–8811.
[137] Sun, M. X.; Cheng, J. M.; Anzai, A.; Kobayashi, H.; Yamauchi, M. Modulating electronic states of Cu in metal–organic frameworks for emerging controllable CH_4/C_2H_4 selectivity in CO_2 electroreduction. *Adv. Sci.* **2024**, *11*, 2404931.
[138] Zhuo, L. L.; Chen, P.; Zheng, K.; Zhang, X. W.; Wu, J. X.; Lin, D. Y.; Liu, S. Y.; Wang, Z. S.; Liu, J. Y.; Zhou, D. D. et al. Flexible cuprous triazolate frameworks as highly stable and efficient electrocatalysts for CO_2 reduction with tunable C_2H_4/CH_4 selectivity. *Angew. Chem., Int. Ed.* **2022**, *61*, e202204967.
[139] Jiao, J. P.; Kang, X. C.; Yang, J. H.; Jia, S. Q.; Peng, Y. G.; Liu, S. Q.; Chen, C. J.; Xing, X. Q.; He, M. Y.; Wu, H. H. et al. Steering the reaction pathway of CO_2 electroreduction by tuning the coordination number of copper catalysts. *J. Am. Chem. Soc.* **2024**, *146*, 15917–15925.
[140] A, B.; Jin, X. X.; Wang, M.; Wang, Y.; Chen, W. R.; Wei, Z. X.; Du, Z. Y.; Liu, X. M.; Wang, Y.; Zhang, L. X. Steering CO_2 electroreduction toward C_{2+} products by defect-engineered coordination microenvironments of Cu-MOFs. *Chem. Eng. J.* **2024**, *500*, 157076.
[141] Deng, J.; Qiu, L. M.; Xin, M. D.; He, W. H.; Zhao, W. H.; Dong, J. C.; Xu, G. T. Boosting electrochemical CO_2 reduction on copper-based metal–organic frameworks via valence and coordination environment modulation. *Small* **2024**, *20*, 2311060.
[142] Liu, Y.; Chen, H. M.; Yang, Y.; Jiao, C.; Zhu, W. K.; Zhang, Y. P.; Wu, X. J.; Mao, J. J.; Zhuo, Z. W. Atomically inner tandem catalysts for electrochemical reduction of carbon dioxide. *Energy Environ. Sci.* **2023**, *16*, 5185–5195.
[143] Lin, L.; Liu, T. F.; Xiao, J. P.; Li, H. F.; Wei, P. F.; Gao, D. F.; Nan, B.; Si, R.; Wang, G. X.; Bao, X. H. Enhancing CO_2 electroreduction to methane with a cobalt phthalocyanine and zinc-nitrogen-carbon tandem catalyst. *Angew. Chem., Int. Ed.* **2020**, *59*, 22408–22413.